nature portfolio

Peer Review File

Force-mediated recruitment and reprogramming of healthy endothelial cells drive vascular lesion growth

REVIEWER COMMENTS

Reviewer #1 (Remarks to the Author):

The paper by Shapeti et al. is very interesting and the data seems quite strong. The question of lesion genesis in CCMs and how variant cells incorporate wild-type cells in malformations is a critical question still not well understood. The assessment of morphological, force-mediated and transcriptomic phenotypes provides a compelling multi-modal analysis in vitro. The findings are, for the most part, well defended and are without a doubt important for the CCM community and potentially the vascular malformation community as a whole. Here are a few major questions, and some minor clarifications, particularly regarding how the findings are grounded within the existing in vivo literature for CCMs and other vascular malformations.

Major Comments:

1) Most importantly, there remains the outstanding question of how consistent the in vitro results are with existing literature on in vivo lesion genesis, where existing work suggests clonal emergence of CCMs and allele frequencies of mutant CCM transcripts are typically <5%. To this end, does data currently exists for the percentage of cells invaded the ECM in the mixed monolayers (10%, 20%, 50%) over time. Are the 50:50 cultures progressively becoming more enriched for wild-type or siCCM cells? How about the other cultures? Further, please provide your understanding of where your findings fit in with in vivo work based on the results of your paper and the existing literature.
2) By eye, the morphology of siCT cells in the CT mosaic cultures in figure 2 appear noticeably distinct from wild-type cells. siCT are an appropriate control for this work and are appropriately assessed in mosaics in figure 2, but figure 1 suggests a morphological difference between siCCM2 and siCT, but does not quantify wild-type. Given the visual difference in siCT cells and WT cells in figure 2, it would be worthwhile to assess the morphological changes induced by transfection alone. Further, the representative image of siCT in figure 1 appears quite linear, whereas the green cells in the figure 2 CT mosaic look bushy, more like siCCM cells in figure 1. Please provide basic morphological characteristics for wild-type cells for the metrics utilized in figure 1.
3) For novel approach to calculating forces, which panels of the main figures are driven by this new approach versus existing approaches? It is not entirely clear where the method from Supplementary note 2 is applied in the main manuscript. Can you apply this method to any publicly available data to assess whether or not the biological interpretation posited is consistent in other in vitro TFM experiments?
4) You suggest "Additional silencing of ROCK1 reverted the increase in ECM displacements and tractions", please provide the statistics between siCCM2 and siCCM2 + ROCK1 or ROCK2 in figure 1, by eye, particularly for tractions, it does not appear there is a clear difference and the mean for siCCM2 + ROCK2 appears lower for both force and tractions in figure 1. To that end, statistics between with and without each ROCK inhibitor versus siCCM2 would provide a better understanding of to what extent each intervention rescues each reported phenotype, particularly force-based phenotypes where the differences appear less dramatic.
5) The model of force mediated recruitment that is suggested appears to be quite specific to CCMs, but low allele frequency is common in nearly all vascular malformations that are seeded by somatic mutation. Would you suggest these findings are specific to lesion genesis in CCMs or would you anticipate similar mechanisms in other vascular malformations?

Minor Comments:
1) For multiple comparisons, Dunn's correction is used instead of Dunnett. Dunnett is more commonly used when comparing to a control group, whereas Dunn is more commonly used for multiple comparisons with no clear control. How do p-values hold up with Dunnett correction? And if using Dunn correction, please include table with statistics

for all comparisons (siCCM2 vs ROCK1 and ROCK2, ROCK1 vs ROCK2 etc) to better understanding the statistical findings
2) Authors suggest a transcriptomic transition to a "stalk-like identity", is a stalk-like identity defined transcriptomically in the existing literature. Is there a set of canonical markers previously shown to be enriched in endothelial cells that behave as stalks? Otherwise it is not clear that the transcriptomic changes are not incidental in regards to the stalk identity.
3) For the transcriptomic analyses, are the siCCM2 cells generated from mosaics as well or are those monolayer siCCM2 cells?
4) %Edu positive cells in figure 4, is that determined by single cell transcriptomic data? It appears to be inconsistent with the staining quantification after 48 hours in extended data 6. Please explain how these figures correspond to each other and include such a discussion in the main manuscript to clarify the finding.

Reviewer #2 (Remarks to the Author):

Title: Force-mediated recruitment and reprogramming of healthy endothelial cells drive vascular lesion growth
Authors: Shapeti et al.

Overview:

The manuscript, entitled "Force-mediated recruitment and reprogramming of healthy endothelial cells drive vascular lesion growth" by Shapeti et al., investigates mechanical mechanisms underlying a vascular abnormality, CCM, using HUVEC 3D cell culture, 3D TFM, and single-cell sequencing. First, the authors examine 3D angiogenic sprouting of the HUVEC in PEG hydrogel, finding that loss of CCM2 enhances angiogenic sprouting potentially through elevated cell-ECM forces and hydrogel matrix degradation via ROCK signaling pathways. Then, they explore the influence of CCM2-silenced ECs on surrounding wild-type ECs and found that WT ECs' invasion modes into the hydrogel are changed by CCM2-silenced ECs and ROCKs. Following that, they investigate the potential mechanisms of this change and claim that hyperactive CCM2-silenced ECs influence WT ECs by potential residual ECM components, pulling forces, and reinforcement of WT EC actin cytoskeleton. Furthermore, the manuscript uses single-cell RNA sequencing to show that CCM2-silenced cells reprogram recruited WT ECs into a proliferative stalk cell identity, indicating a potential mechanically-driven cell reprogramming.

Mechanics has proven vital in various biological processes such as morphogenesis and angiogenesis, as well as in the pathogenesis of diseases like cancer and cardiovascular diseases. Yet, the exploration of mechanics in vascular diseases, particularly within cerebral systems, remains limited. This work delves into a compelling topic by investigating the mechanical mechanisms involved in vascular diseases, offering potential insights into the role of mechanics in tissue heterogeneity and disease progression. This research has the potential to gain significant attention from the field. However, some of the conclusions do not yet appear to be justified by the data. Therefore, we offer the following comments that should be addressed.

Major Comments:

Overall, the manuscript needs improvements to draw its conclusions because of the following concerns.

1. The manuscript lacks clarity in the description of the 3D models used, limiting the potential for reproducibility. The authors use schematics to describe their experiment

setups, such as Figs. 1a, 2a, 3a etc., but there is no single image showing the real setups. Providing a clear depiction of experimental setups, including details such as device images, hydrogel thickness, and a 3D schematic of the device with scale bars, would enhance the transparency and replicability of the study. Moreover, in reference 59 where the authors describe their model, it is somewhat unclear whether the sprouts are extending on top of the gel or penetrating into it. Fig. 1a,b in that paper appear to show sprouts on top of the gel.
2. In the present paper, the authors have changed from using collagen to a functionalized PEG gel. This differs from true extracellular matrix in several important aspects: 1) The mesh spacng in a PEG gel is much smaller than in collagen, for example. Hence the sprouting (assuming it penetrates the gel) requires matrix degradation to occur whereas in other, perhaps more physiological gels, the interfiber spacing could be sufficiently large to allow filipodia to extend without degradation. 2) Also due to the small mesh spacing, diffusion of signaling molecules could be impeded relative to in vivo. This might accenuate the effects of mechanical signaling due to suppression of biochemical signaling. 3) While real ECM would be degraded by a wide range of MMPs, the PEG gel used here appears to have just one MMP-cleavable linkage. Thus, statements regarding the role of a single integrin or MMP may not be generalizable.
All this leads to the point that the authors need to provide a deeper discussion of their choice of gel and the potential artifacts associated with it. Their results specifically pertain to a gel with particular cleavage and adhesion proteins tethered to the matrix.
3. The manuscript lacks validation through raw 3D images. For example, validation of the claims of this manuscript depends on their relevant 3D network structures, but there are no 3D images (e.g., confocal imaging) to confirm that, such as how thick are the networks, what are the dimensions of the lumens if they exist, etc. Another example is that they only showed local mosaic images, without any sprouting network images in one big device, making it difficult to acertain the influence of how they select the samples on the final analysis of the results.
4. The manuscript lacks percentage comparison details. The manuscript relies on percentage comparisons without providing the necessary context such as absolute numbers, variations among cells, etc. Examples are:
a. In Result 3, “Remarkably, we observed that 80% of invading WT ECs in CCM2 mutant mosaics…”. This statement lacks context without absolute numbers of cells in each mode. It's crucial to present these numbers to fully understand the percentage comparisons here. For instance, in Fig. 2g, the 0% of invading WT ECs classified as Mosaic Stalkers in CT mosaics can be misleading since there are no CCM2-silenced cells in this group, resulting in a total count of zero. A comparison between groups like CCM2 and CCM2-ROCK1 also necessitates the inclusion of absolute numbers for a valid comparison.
b. In Result 4, “Strikingly, WT ECs in mutant mosaics regain tip cell behavior when either ROCK1 or ROCK2 is depleted in the siCCM2 EC”. The total numbers of cells exhibiting this behavior need to be provided to substantiate this claim.
a. In Result 5, “Taken together, this establishes that CCM2 loss drives a ROCKs-dependent non-autonomous inhibition of leader cell behavior in WT ECs”. The total numbers of cells exhibiting this behavior need to be provided to substantiate this claim.
5. Please clarify Sample Numbers (n). The meaning of sample size (n) is unclear. Is it device numbers or cell numbers? If cell numbers are used for comparison, further evidence of small variations among devices and overview images of sprouts are needed.
6. The claim that CCM2-silenced ECs lead 80% of WT ECs as "mosaic stalkers" lacks validity. The authors did not investigate whether the CCM2 ECs also induce changes in other CCM2 ECs. The observed alterations may stem solely from the adherence of wild-type (WT) ECs to the CCM2 ECs, potentially indicating a passive influence (that the CCM2 ECs are simply dragging the WT ECs along) rather than a positive regulatory effect. Further elucidation is required to provide a more comprehensive understanding of this phenomenon.
7. The manuscript lacks proof of the WT EC contribution. The manuscript lacks evidence proving the contribution of WT ECs to true multi-cellular angiogenic sprouting as

opposed to 1-2 cell migration/protrusion, limiting the impact of the work. Longer-term cell cultures might be used to prove the impact of WT ECs on angiogenesis.
8. The Supplementary Text, especially the equations, has somehow been distorted in the file we received, so it would be helpful to receive another version of that.

Minor Comments:

1. In the abstract, the phrase "Here, we use 3D traction..." should be revised to "Here, we utilize an in-vitro model involving 3D traction..."
2. In Fig 1, it is necessary to provide a rationale for the significantly higher variations observed in the siCCM2 groups compared to other groups.
3. In Fig. 1b, while only the first and third images currently depict the monolayer morphology, it would be beneficial to include monolayer representations for the second and fourth images for consistency and clarity. This suggestion applies similarly to Figure 3b.
4. The absence of overview images in the paper, particularly where percentages are used to substantiate claims (such as in Figure 2g), is a limitation. Without comparing the entire structures across different groups, relying solely on percentage comparisons may lead to misinterpretations or incomplete conclusions.
5. In Result 1, the discussion around Rho-associated coiled-coil forming protein kinases (ROCKs) requires a more detailed explanation, especially for readers who may not be familiar with this topic. Clarifying why ROCKs were specifically chosen for this study would make the results more accessible to a broader audience.
6. In Result 2, "Surprisingly, the numerous filopodia still observed in siCCM2+siROCK2 sprouts did not translate to higher forces on the ECM (Fig 1d,e)." The role of myosin II and its relationship with ROCK in force generation should be also considered. Highlighting that more actin doesn't necessarily equate to higher forces could clarify why this observation might not be as surprising.
7. In Result 2, more explanation of MT1-MMP is needed for a broader audience.
8. In Result 5, the statement "When observing invasion dynamics, we often noted that hyper-migratory siCCM2 tip cells…" requires quantification of the term "often." Additionally, providing a histogram or similar graphical representation in relation to Figure 3g would substantiate the claim with concrete data.
9. In Discussion, consider exploring the possibility that CCM2-silenced cells exhibit increased adhesion, causing surrounding cells to adhere and move with them. This alternative hypothesis could provide a different perspective on the observed behaviors.
10. In Discussion, it would be beneficial to critically evaluate whether the observed phenomena should be characterized as mechanical signals or simply as a result of physical forces. This distinction is important for accurately interpreting the study's findings.

Reviewer #3 (Remarks to the Author):

I co-reviewed this manuscript with one of the reviewers who provided the listed reports. This is part of the Nature Communications initiative to facilitate training in peer review and to provide appropriate recognition for Early Career Researchers who co-review manuscripts.

We would like to thank the reviewers for their critical review of our work and for providing valuable remarks that have helped improve the quality and impact of this study. We have carefully considered the concerns and included a point by point response to each of the comments. Where relevant, we have included additional quantifications, figures, schematics and experiments in the updated manuscript to further clarify these concerns. All changes in the text are highlighted in a blue font.

Reviewer #1 (Remarks to the Author):

The paper by Shapeti et al. is very interesting and the data seems quite strong. The question of lesion genesis in CCMs and how variant cells incorporate wild-type cells in malformations is a critical question still not well understood. The assessment of morphological, force-mediated and transcriptomic phenotypes provides a compelling multi-modal analysis in vitro. The findings are, for the most part, well defended and are without a doubt important for the CCM community and potentially the vascular malformation community as a whole. Here are a few major questions, and some minor clarifications, particularly regarding how the findings are grounded within the existing in vivo literature for CCMs and other vascular malformations.

Major Comments:

1. **Most importantly, there remains the outstanding question of how consistent the in vitro results are with existing literature on in vivo lesion genesis, where existing work suggests clonal emergence of CCMs and allele frequencies of mutant CCM transcripts are typically <5%. To this end, does data currently exists for the percentage of cells invaded the ECM in the mixed monolayers (10%, 20%, 50%) over time. Are the 50:50 cultures progressively becoming more enriched for wild-type or siCCM cells? How about the other cultures? Further, please provide your understanding of where your findings fit in with in vivo work based on the results of your paper and the existing literature.**

   We would like to thank Reviewer 1 for this important comment. Indeed, the previously identified allele frequencies of somatic mutations in familial and sporadic CCMs is found to be <10% [1,2]. In mice, Dejana's group showed that mutant endothelial cells (ECs) first clonally proliferate, which is then followed by a progressive enrichment of wild-type (WT) ECs to expand the lesions [3]. At P30, confetti mice lesions contained 60% WTs. Also, when $CCM3^{-/-}$ cells were grafted in wild-type mice brain, they started to show abnormal vessel formation with a recruitment of wild type ECs from the host brain.

   At P8, lesions in mice contained only 10% WT cells, which increased to 60% by P30. Our conditions containing 80 and 90% WTs (10%, 20% siCCM2) would be comparable to later stage, older, mature lesions. Since we did not see secondary effects on WT ECs in the 10% condition, our findings would suggest that recruiting capacities of mutant cells at this late stage of the lesion might be limited. This was our reasoning for choosing the 50-50% cultures as a model for less mature growing lesions where we sought to observe the mechanisms involved in incremental WT EC recruitment and the modification of their behavior. To this end, we performed timelapse imaging of these mixed populations during mosaic sprouting to study the enrichment of WT ECs over time.

   To further illustrate that indeed the 50:50 cultures became more enriched for wild-type ECs over time, we added two additional quantifications to the manuscript in Fig.2 based on the 18h overnight films. We were unable to timelapse image nuclei using Hoechst because of phototoxicity from the UV in large 3D stacks. To circumvent this, we chose to quantify the area occupied by each cell type over time as a substitute for cell numbers (Fig. 2f). As a measure of their relative

enrichment with time, we also represented this as relative percentages of area covered by siCCM2 mutants and wild-types (Fig. 2g). Further, we also quantified the number of nuclei for mutant versus WT ECs in mosaic sprouts observed after 18h of invasion (Fig. 2h). This gives an estimate of the number of WT cells that followed behind leading siCCM2 ECs.

Based on these new quantifications, we found that both siCCM2 and WT ECs were enriched with time in the gels, as seen in the area occupied by them in **Error! Reference source not found.**. Consistent with the previously quantified invasion distance over time, WT ECs are delayed in invading the matrix confirming that the mutant ECs have an invasive advantage. After this initial delay, WT ECs begin to progressively occupy more area of the matrix. Moreover, there is an increase in the percentage of area occupied by WT versus siCCM2 ECs with time as shown in **Error! Reference source not found.** 2g, showing that WTs get enriched once the highly invasive mutant tips have migrated forward. Finally, when looking at the mosaic sprouts at the end of the experiment after 18h, we saw a ratio of 1 CCM mutant for 3 WT ECs (Fig. 2h).

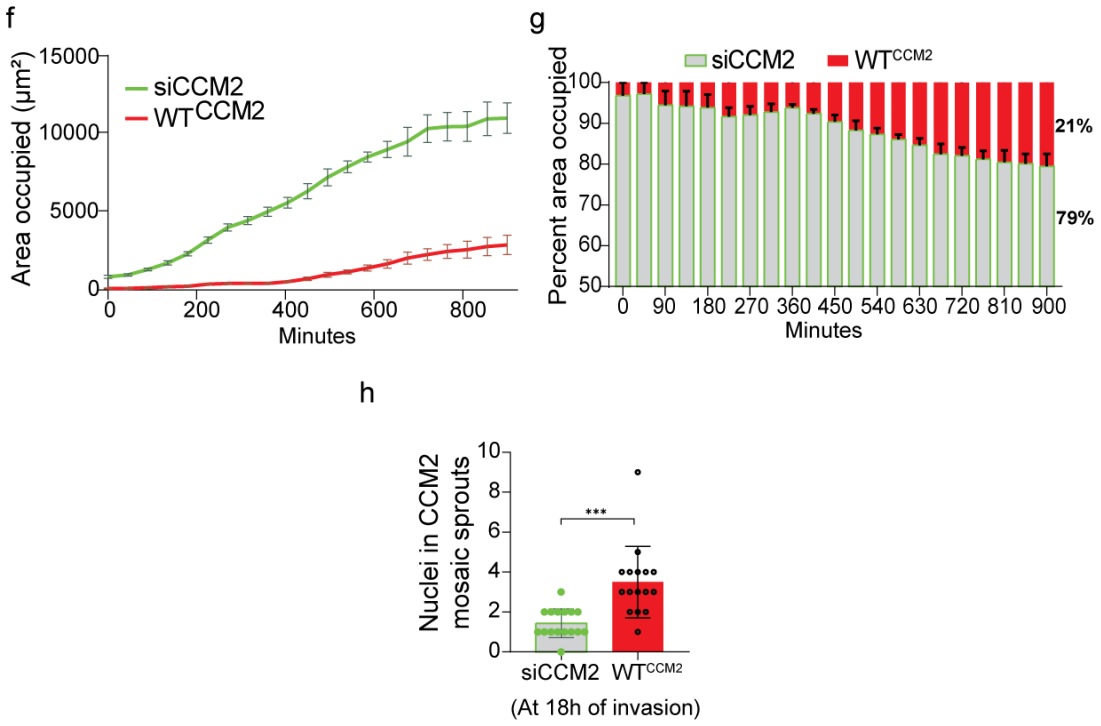

Fig. 2: **f.** Automated quantification of the progressive area of the matrix occupied by each cell type in CCM2 mutant mosaics. **g.** Relative matrix area occupied by each WT or siCCM2 ECs in CCM2 mosaics showing WT enrichment over time. **h.** Number of nuclei quantified in mosaic sprouts composed of WT and siCCM2 ECs after 18h of invasion in CCM2 mutant mosaics. 2 independent trials with a total of 16 mosaic sprouts compared using a Wilcoxon test.

We would again like to thank the reviewer for this comment as it has allowed us to emphasize the progressive enrichment of WT ECs in the sprouts as seen in the context of in-vivo lesions. We have now adapted the text in the results section of the manuscript to reflect the answers to these comments in lines 158 to 181 as follows:

> *"To further explore angiogenic activation of WT ECs by CCM mutants, we visualized collective sprouting in two situations (Fig. 2a): (i) CT mosaics where LifeAct-RFP tagged WT ECs were mixed with LifeAct-GFP tagged siCT ECs, and (ii) CCM2 mosaics where LifeAct-RFP tagged WT ECs were mixed with LifeAct-GFP tagged siCCM2 ECs in various percentages. Late stage symptomatic lesions are found to contain only 10-20% mutant ECs*[3–6]*. In mice, Dejana's group*

showed that mutant ECs first clonally proliferate, which is then followed by a progressive enrichment of WT ECs to expand the lesions[3]*. At P8, lesions contained only 10% WT cells which increased to 60% by P30. By varying percentages of silenced ECs in mosaics (Fig. 2a), we noted an increase in invasion of WT ECs in CCM2 mutant mosaics composed of 50% and 20% siCCM2 ECs, but not at 10% (Fig. 2b). This implied that a minimum critical mass of siCCM2 ECs was necessary in our model to modify angiogenic behavior of neighboring WT ECs.*

Our conditions containing 80 and 90% WTs (10%, 20% siCCM2) would be comparable to in vivo later stage lesions. Since we did not see effects on WT ECs in the 10% condition, our findings would suggest that recruiting capacities of mutant cells at this late stage of the lesion might be limited. Hence, we chose 50-50% cultures to model less mature lesions, which we used for all further mosaic studies. To this end, we performed timelapse imaging of these mixed populations during mosaic sprouting. Tracking dynamics of angiogenic sprouting over 18h showed that both siCCM2 and WT ECs begin invading earlier and faster in CCM2 mutant mosaics than in CT mosaics (Fig. 2c-e, Supplementary Videos 2A-B). However, siCCM2 ECs initiated invasion earlier than the WT ECs in these CCM2 mutant mosaics and had an invasive advantage as shown by their increased invasion speed (Fig. 2d,e). Further, we saw an enrichment of both siCCM2 and WT ECs with time in the gels, as seen with the matrix area occupied by them in Fig. 2f. Consistent with Fig. 2c, WT ECs were delayed in invading the matrix confirming the invasive advantage of mutant ECs. After this initial delay, WT ECs began to progressively occupy more area of the matrix. Moreover, there was an increase in the relative area occupied by WT versus siCCM2 ECs with time (Fig. 2g), showing that WTs got enriched once the highly invasive mutant tips had migrated forward. Finally, when looking at mosaic sprouts at the end of the experiment after 18h, we saw a ratio of 1 CCM mutant for every 3 WT ECs (Fig. 2h). This was consistent with in vitro findings where CCM spheroids got enriched with WT ECs from neighboring monolayers[3]*."*

2. **By eye, the morphology of siCT cells in the CT mosaic cultures in figure 2 appear noticeably distinct from wild-type cells. siCT are an appropriate control for this work and are appropriately assessed in mosaics in figure 2, but figure 1 suggests a morphological difference between siCCM2 and siCT, but does not quantify wild-type. Given the visual difference in siCT cells and WT cells in figure 2, it would be worthwhile to assess the morphological changes induced by transfection alone. Further, the representative image of siCT in figure 1 appears quite linear, whereas the green cells in the figure 2 CT mosaic look bushy, more like siCCM cells in figure 1. Please provide basic morphological characteristics for wild-type cells for the metrics utilized in figure 1.**

We thank reviewer 1 for this interesting remark. Indeed, we consistently observed that the steps of siRNA transfection reduced the robustness of the angiogenic response in siCT cells when compared to WT ECs. For any given combination of ECM stiffness and S1P concentration, we noticed that the siCT ECs always showed decreased invasion relative to WT ECs. We have now added a baseline experiment comparing the morphology and invasion of siCT and WT ECs and have added this to Extended Data Fig. 1. We found that there was no significant difference in the filopodial morphology metrics between transfected and non-transfected ECs (Extended Data Fig. 1C). However, we observed a significant increase in the invasion distance of WT ECs relative to siCT ECs. We also included an overall invasion image of the monolayer showing this in Extended Data Fig. 1B. This finding even further emphasizes the hyperangiogenic capacities of the siCCM2 ECs which undergo the same transfection protocol. Indeed, despite this handicap, siCCM2 ECs are capable of outcompeting robust WT ECs to take the lead and to recruit them into mosaic lesions as stalk cells. The new quantifications are shown below:

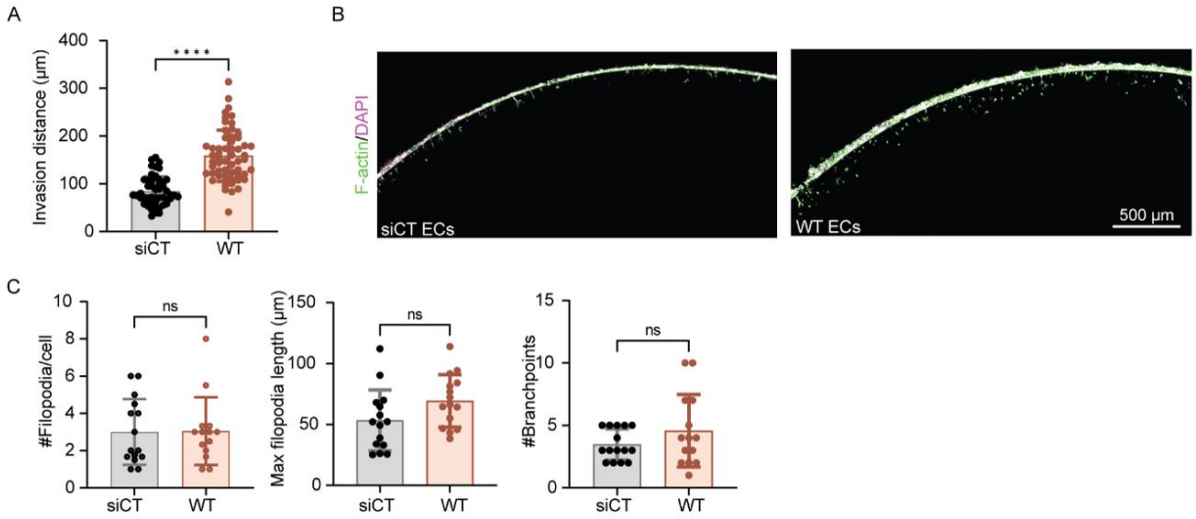

Extended Data Fig. 1: **siRNA transfection reduces robustness of invasion. A.** Quantification of maximum invasion distance over 1 invading monolayer of siCT ECs versus WT ECs. **B.** Maximally projected sprouting confocal images of siCT versus WT ECs after 18h of invasion over a 100 µm thick stack. **C.** Filopodial morphological metrics in leading tip regions for an n=15 from 1 independent trial for both conditions.

We have adapted the text to refer to these findings as follows:

Lines 84 to 93:

*"siRNA silencing of CCM2 in EC monolayers previously showed ROCK1-dependent increased angiogenic invasion compared to siCT ECs in this model*30*. siRNA transfection alone affects the robustness of invasion which can be seen in Extended Data Fig. 1A,B. This however, only further emphasizes the hyper-angiogenic capacities of the siCCM2 cells which also undergo the same transfection protocol. Given that filopodia are known to guide endothelial tip cells towards angiogenic stimuli*31,32*, we wondered if these structures were altered in response to CCM2 loss. Upon closer examination, we observed that highly angiogenic CCM2-silenced sprouts, referred to as siCCM2 ECs, (Fig. 1b), exhibited denser localization of F-actin (Fig. 1b,d) and a pronounced branchy tip cell phenotype*32 *characterized by longer filopodia compared to control sprouts, denoted as siCT (Fig. 1b,c). Despite the reduced invasion of siCT ECs compared to non-transfected ECs (Extended Data Fig. 1A,B), siRNA transfection did not significantly affect filopodia formation in siCT ECs (Extended Data Fig. 1C)."*

Lines 187 to 190:

"In contrast, WT ECs in CT mosaics begin invading the matrix mainly as "lone tips" and never assume "mosaic stalk" positions (Fig. 2c,j), suggesting that CCM2 mutant ECs are capable of inhibiting a tip phenotype in WT ECs. We concluded that siCCM2 cells are capable of outcompeting WT cells to take tip cells position and recruiting them into mosaic invasion."

Regarding the differences in siCT morphology between Fig. 1 and Fig. 2, we believe it comes from difference in imaging the stacks. Overnight imaging in Fig2 was performed at a lower resolution and magnification, higher laser power and a larger z-stack to provide an overview of the invasion dynamics and to ensure the visualization of all migrating structures than in Fig1. As such, this dataset is a maximum intensity projection of a 100um z-stack projecting multiple invading protrusions over different z planes. As a result, there is a mismatch between the high resolution and high magnification images capturing only an individual sprout in Fig. 1 versus those in Fig. 2. To clarify this, a sentence has been added to the methods section detailing overnight invasion imaging for cell tracking in lines 801 to 807 as follows:

"*Confocal images stacks (100µm thick, 1 µm step size) of mosaic sprouting acquired every 45 minutes over 16 hours were used to visualize dynamic imaging. These images were captured at a 3 times lower resolution and magnification than those acquired for visualizing the filopodia morphology in Fig 1b. Further, they captured a large z-stack resulting in overlay of multiple sprouts in the maximal intensity projected videos. As a result, these images should be used for studying dynamics but not morphometric analysis. To track cell dynamics for invasion and area quantifications, the images were first maximally projected in ImageJ and converted to .avi files in RGD format*."

3. **For novel approach to calculating forces, which panels of the main figures are driven by this new approach versus existing approaches? It is not entirely clear where the method from Supplementary note 2 is applied in the main manuscript. Can you apply this method to any publicly available data to assess whether or not the biological interpretation posited is consistent in other in vitro TFM experiments?**

The existing 3D TFM approach gives the results in Figure 1 (panels g,h and f) and Figure 3 (panels b, d, e and f). We presented this approach in earlier publications [10–12] and described it in Supplementary Note 1. Briefly, we first measure the displacements of the ECM comparing the bead images before and after cell relaxation with Cytochalasin-D. Based on these measurements we then quantify cell-ECM tractions. However, this approach alone does not provide information on cell-cell forces.

The novel development in this paper involves using the calculated cell-ECM tractions to infer the resultant cell-cell force occurring at the interface of a cell pair. This is the approach described in Supplementary Note 2 and is applied to compute the results shown in Figure 3h. To clarify this, we have now explicitly mentioned it in the caption of Figure 3h as follows:

> ***"h.*** *Novel approach to compute average forces at a 3D interface of a cell pair, as detailed in Supplementary Note 2.* (***left***) *Schematic of a mosaic cell pair depicting the two cell-hydrogel interfaces (green, Ω_1; red, Ω_2), the cell-cell interface (yellow, Ω_3), forces exerted by the cells on the hydrogel (**F**), and the force balance equation to quantify resultant force on the interface."*

We have also highlighted the instances in the results section where the method is referred to (in cyan). This can be found in Lines 237 to 247 and is as follows:

> "*Therefore, to evaluate if leading siCCM2 ECs were mechanically interacting with stalk WT ECs at cell-cell contacts, we developed a novel 3D TFM approach based on first principles, i.e. linear and angular momentum conservation [13], to quantify the resultant (net) force at this interface (Fig. 3h, Supplementary Note 2). By recovering the forces exerted on the ECM by a detached cell pair of a siCCM2 leader and a WT follower, we found that the average cell-ECM traction exerted by the mutant tip largely exceeded that by the WT stalk (Fig. 3h, Table 1 in Supplementary Note 2). Further, quantifying the resultant cell-cell force vector at the interface between these cells showed a substantial, non-zero force (~14 nN) and corresponding average cell-cell traction (~7 pN/µm^2), indicating that the two cell types mechanically interact by means of pulling forces. Given that the resultant force from the tip cell on the stalk cell was aligned with the direction of migration of the cell pair (see Fig 3h), we deduced that these cell-cell pulling forces are important for bringing the WT stalk forward and to ensure collective*

migration of the tip and stalk cell (see detailed interpretation presented in Supplementary Note 2).”

We thank the reviewer for the second comment which we find highly stimulating. It would indeed be very interesting to apply this approach to existing datasets from 3D TFM exploring other biological questions. A current limitation for this is, to the best of our knowledge, a lack of appropriate datasets of this nature. 3D TFM, although powerful, remains an underused technique due to its complexity, as a result of which there aren't enough datasets publicly available. To counter this, we are currently preparing a protocol manuscript to simplify this technique for broader adoption. Further, applying this approach requires that cells are labeled with different fluorescent markers so that their interface can be appropriately segmented in 3D. This is a prerequisite to computing the force at the interface of cell pairs. Most previous TFM studies with multiple cell populations have used the technique only in 2D. We hope to apply this method in the future to more such datasets to further uncover processes driven by intercellular force transmission in 3D.

4. **You suggest “Additional silencing of ROCK1 reverted the increase in ECM displacements and tractions”, please provide the statistics between siCCM2 and siCCM2 + ROCK1 or ROCK2 in figure 1, by eye, particularly for tractions, it does not appear there is a clear difference and the mean for siCCM2 + ROCK2 appears lower for both force and tractions in figure 1. To that end, statistics between with and without each ROCK inhibitor versus siCCM2 would provide a better understanding of to what extent each intervention rescues each reported phenotype, particularly force-based phenotypes where the differences appear less dramatic.**

We have now updated the statistical analysis to include comparisons between siCCM2 and both siCCM2+ROCK1 and siCCM2+ROCK2 conditions for both displacements and tractions. A table reflecting each of the p-values is shown here below. We have also performed statistics between with and without each ROCK silencing versus siCCM2 for every quantification in the paper, and further clarified this in the figure captions. Detailed tables of all comparisons and p values are included in the “Source Data” sheet.

Table 1: 90th percentile displacements and tractions (original metric used)

Kruskal Wallis with Dunn's correction	Displacements (µm, 90th percentile)	Tractions (Pa, 90th percentile)
siCT vs *siCCM2*	0,0033 (**)	0.0026 (**)
siCT vs *siCCM2+ROCK1*	>0,9999 (ns)	0.2336 (ns)
siCT vs *siCCM2+ROCK2*	>0,9999 (ns)	>0,9999 (ns)
siCCM2 vs *siCCM2+ROCK1*	0,0008 (***)	0,5289 (ns)
siCCM2 vs *siCCM2+ROCK2*	<0,0001 (****)	0,0141 (*)

Based on the p values for the 90th percentile displacements and tractions (originally used metric in the manuscript), ROCK2 silencing has a stronger effect on rescuing forces at the tip of the ROCK1-dependent filopodia. When comparing the displacements, ROCK1 still also rescues this effect, consistent with the fewer filopodia. However, the differences observed when comparing tractions versus displacements are much smaller for siCCM2+ROCK1 versus siCCM2. This is an important difference we had not previously noted, and we thank the reviewer for pointing this out as this has led us to a much better understanding of the usefulness of various metrics in 3D TFM.

We further sought to understand the source of this discrepancy between the two metrics. We found this to be driven by two factors which we describe below:

1. Our initially selected criteria for reporting both displacements and tractions was the 90th percentile, which was based solely on the displacement histogram. We did not report the maximum in order to prevent misinterpretation from noisy outliers. However, we now plotted the histograms for the magnitude of the displacements as well as the tractions at the nodes of the cell surface and discovered that the two distributions vary strongly (see Report Fig.1).

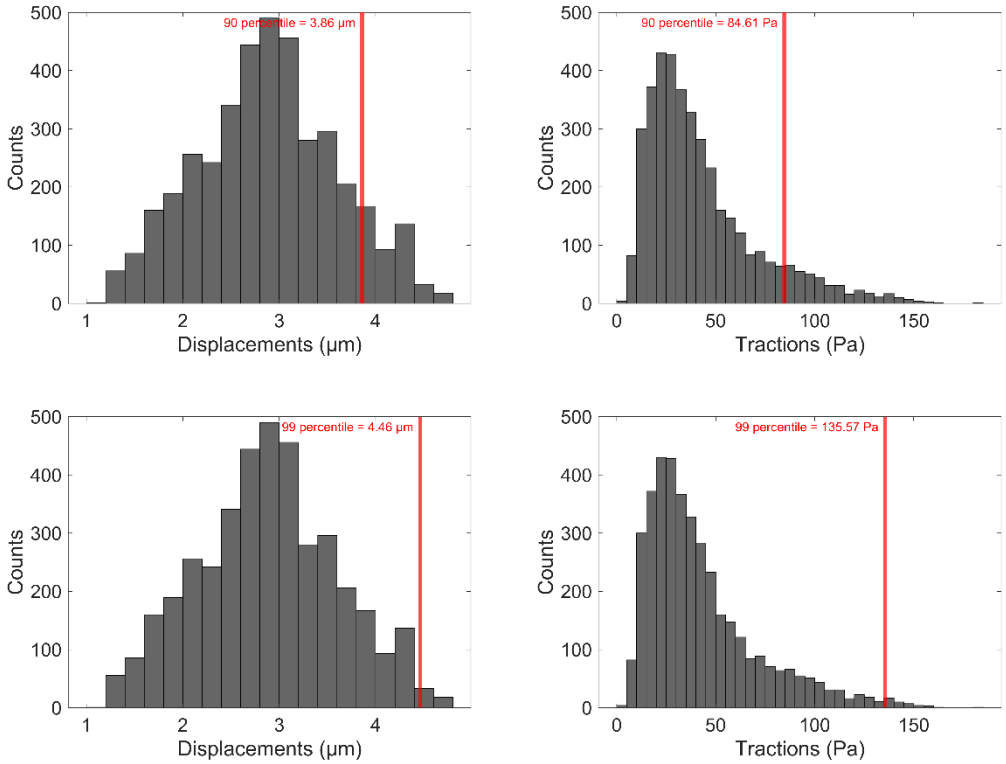

Report Fig. 1: Representative histograms of displacements and tractions

The displacement histogram has a normal-like distribution that decays relatively smoothly towards higher magnitude values. However, the traction histogram has its peak closer to low values and rapidly decays towards high values. Tractions are naturally sparse, with the cell exerting high forces only at a few points. This inherent difference leads to a higher sensitivity of the tractions to the percentile value chosen. As can be seen in the figure below, the 90th percentile of the tractions is 84.61 Pa, which is still far from the higher values that the cell is able to exert (which lie within the range of 120-150Pa). However, by increasing the percentile to 99th we obtain a value that better captures the high tractions, namely 135.57 Pa. For the displacements, because of their smooth decay, the change of percentile does not vary the obtained value significantly (3.86 vs 4.46 microns). We also provide the histogram of the tractions with logarithmic Y-axis to aid the visualization of its higher values (see Report Fig. 2 below).

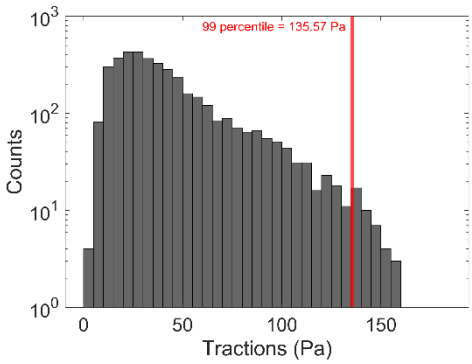

Report Fig. 2: Representative histograms of displacements and tractions

As a result, choosing the 90th percentile metric for tractions resulted in an underestimation of the peak tractions, whereas this metric did not lead to such effects in the case of displacements. We now reported the 99th percentile for both parameters and have updated the figures in the manuscript and also include the subsequent statistical analysis in the table here below.

Table 2: 99th percentile displacements and tractions (updated metric now used)

Kruskal Wallis with Dunn's correction	**Displacements** (µm, **99th percentile**)	**Tractions** (Pa, **99th percentile**)
siCT vs *siCCM2*	0,0017 (**)	0,0147 (*)
siCT vs *siCCM2+ROCK1*	>0,9999 (ns)	>0,9999 (ns)
siCT vs *siCCM2+ROCK2*	>0,9999 (ns)	>0,9999 (ns)
siCCM2 vs *siCCM2+ROCK1*	0,0004 (***)	0,2121 (ns)
siCCM2 vs *siCCM2+ROCK2*	<0,0001 (****)	0,0069 (**)

2. Secondly, tractions are a measure of a force per unit area exerted by individual local force exerting regions on a sprout tip. As such, a measure of the peak tractions does not necessarily represent the overall force exerting capacity of the cell itself. As a result, we decided to additionally report the strain energy, which is also a commonly used metric in TFM [14–16]. It is a measure of the work done by the cell to deform the matrix. The strain energy was calculated as follows:

$$Energy = \frac{1}{A_{tot}} \sum \boldsymbol{f}_i \cdot \boldsymbol{u}_i$$

where $\boldsymbol{f}_i$ and $\boldsymbol{u}_i$ are the nodal force and displacement vectors, respectively, computed at the node i of the surface mesh of the cell. A_{tot} is the total surface area of the cell tip.

This quantification is now added to manuscript Fig. 1 and the Supplementary Note 1 as shown above in Lines 174 to 180. When statistically comparing the strain energy and thereby the overall force generation by sprout tips, it becomes evident that both ROCK1 and ROCK2 depletions are able to rescue force-based phenotypes. ROCK2 nevertheless has a stronger influence on force generation as seen in the increased significance. This is shown in the table below and added to the text as well:

Table 3: Strain energy comparisons (Pa um) (newly added metric, measure of total work done by the cell)

Kruskal Wallis with Dunn's correction	**Strain Energy (Pa um)**
siCT vs *siCCM2*	0,0005 (***)

siCT vs *siCCM2+ROCK1*	>0,9999 (ns)
siCT vs *siCCM2+ROCK2*	>0,9999 (ns)
siCCM2 vs *siCCM2+ROCK1*	0,0011 (**)
siCCM2 vs *siCCM2+ROCK2*	<0,0001 (****)

The updated quantifications are shown below:

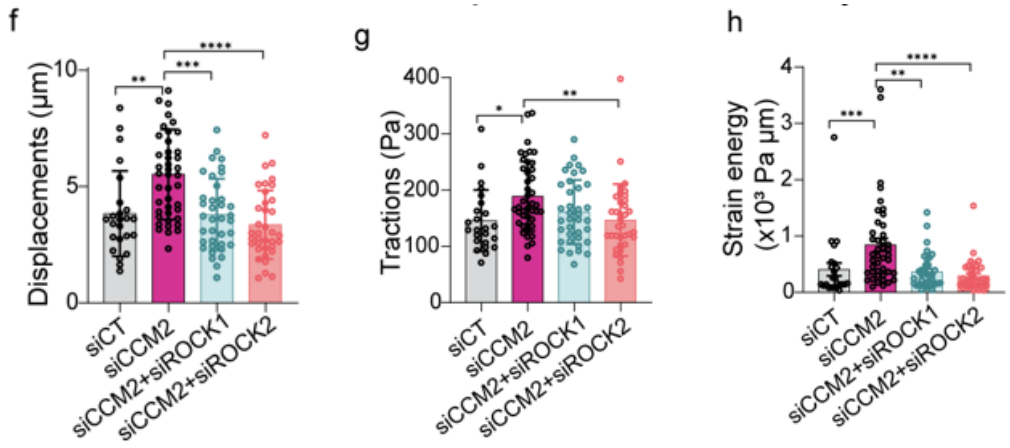

Fig. 1: f-h. Automated quantification of the 99th percentile bead displacements (f, in µm) and tractions (g, in Pa), and strain energy (h, in Pa µm) exerted by force exerting sprout tip regions (3 independent trials; siCT, n=24; siCCM2, n=43; siCCM2+ROCK1, n=37; siCCM2+ROCK2, n=35).

We adapted the text in the results section in Lines 113 to 126 to reflect our findings:

> *"As predicted, siCCM2 sprout tips pulled more strongly on the ECM to generate 45% higher bead displacements and 20% higher subsequent tractions on the ECM compared to siCT sprout tips (Fig. 1e-g). This is further supported by a twofold increase in the strain energy of siCCM2 tips (Fig. 1h). Additional silencing of ROCK1 reverted the increase in ECM displacements and strain energy, and partially lowered tractions. This was consistent with the decrease in filopodia upon ROCK1 depletion, as previously observed in dendritic cells where ROCK1 was necessary for Rac1-dependent filopodia at the front (Fig. 1b,c)[17]. Taken together, this suggests that tractions exerted by siCCM2 ECs were associated with the abundant ROCK1-dependent tip cell filopodia. Surprisingly, the highly invasive siCCM2+siROCK2 sprouts with their numerous filopodia did not generate higher forces on the ECM (Fig. e-h), suggesting a lack of myosin II-dependent contractility. Interestingly, ROCK2 was previously reported to generate contractile force at filopodia through the phosphorylation of myosin-light chain and cofilin in dendritic spines[17]. Consistently, we found that ROCK2 silencing had a stronger effect on rescuing forces than ROCK1 at the numerous ROCK1-dependent filopodia, as is visible in the lower displacements, tractions and strain energies. However, a complete restoration of the increased forces observed upon CCM2 loss seemed contradictory with the sustained increase in invasiveness and F-actin of these siCCM2+siROCK2 sprouts (Fig 1b,d)."*

5. **The model of force mediated recruitment that is suggested appears to be quite specific to CCMs, but low allele frequency is common in nearly all vascular malformations that are seeded by somatic mutation. Would you suggest these findings are specific to lesion genesis in CCMs or would you anticipate similar mechanisms in other vascular malformations?**

We thank the reviewer for yet another highly stimulating comment. This comment led us to explore the existing literature on vascular malformations for mechanistic similarities with CCM pathogenesis. Interestingly, various malformations seeded by somatic mutations indeed show low allele frequency and also present with similarly dysregulated angiogenic pathways. Based on this, we would hypothesize that our identified mechanisms might also be one of the underlying mechanisms for the pathophysiology of other vascular anomalies. We discuss below some of the key evidence supporting this for specific vascular malformations:

Sturge Weber Syndrome (SWS): These capillary malformations are associated with causative activating somatic mutations in the GNAQ genes and are a congenital low flow malformation associated with numerous dilated capillaries – similar to CCMs [18]. These vessels are known to overexpress KDR (kinase insert domain receptor) which is a receptor for VEGF-A to promote vascular migration and permeability, suggesting increased angiogenic phenotypes [19]. Further, Gαq proteins can also enhance VEGF-induced EC migration by facilitating activation of RhoA and Rac1, as well as calcium channel mechanosensing signaling pathways [19]. In addition to these upregulated angiogenic and mechanosignaling pathways in common with CCM, SWS affected tissues show a variant allele frequency of <18% suggesting a potential role for non-mutant cells [18].

PI3K-associated vascular lesions: Mutations in genes like PIK3CA or NRAS are frequent in lymphatic malformations, causing hyper-branching, sprouting and vessel overgrowth. Interestingly, the PIK3CA mutation is carried by only a fraction of the lymphatic ECs, necessitating other strategies for LM lesion growth. Experts in the field have recently hypothesized that a small population of mutant clones might use clonal cooperation to signal to normal ECs in the neighboring regions leading to their potential functional alteration [20]. Further, a new PI3K-driven lesion model described in the postnatal mouse retina has shown that active angiogenesis is a prerequisite for the pathogenesis of malformations caused by PIK3CA activating mutations [21]. While mechanics has not yet been proposed as a direct factor contributing to PI3K-lesions, the similarly upregulated angiogenic pathways as in CCMs and the hypersprouting phenotypes might suggest an involvement of similar mechanically mediated recruitment contributing to the clonal cooperation.

Hereditary hemorrhagic telangiectasia (HHT): HHT1 and HHT2 are the main disease causing variants of HHT with heterozygous mutations in endoglin, activin receptor-like kinase 1 (ALK1) or SMAD4. Loss of function of encoded proteins can lead to vascular overgrowth from the overactivation of PI3K signaling [22]. Like in CCM, ALK1-depleted ECs display high migratory and invasive behaviors, and an enhanced response and sensitivity to proangiogenic cues [22]. However, most vessels of HHT patients are without pathological lesions, suggesting that ALK1 heterozygous ECs may require an additional somatic mutation or environmental stressor such as a local angiogenic stimulus [23]. This combined with the fact that affected tissues show low variant allele frequency suggest significant overlapping pathways with CCM pathophysiology.

Introduction: we have now included an additional section in Lines 58 to 64 to introduce this context to vascular malformations. This is included here below:

> *"In advanced stages, symptomatic CCM lesions manifest as hemorrhagic, multicavernous structures comprising both mutant and wild-type (WT) ECs*10–14*. Interestingly, various other vascular anomalies such as Sturge Weber Syndrome (SWS), PI3K-driven vascular and lymphatic malformations and hereditary hemorrhagic telangiectasia (HHT), also present mosaic lesions and show similar overactivation of angiogenic pathways*[18,19,21–23,26]*. As CCM lesions expand, mutant cells attract WT ECs into the growing lesions*8,9*, making this step in CCM formation a crucial therapeutic target for reducing symptoms. The precise mechanisms underlying this*

recruitment remain unknown and could be relevant for the growth of other mosaic vascular malformations as well."

Discussion: We have also added our reflection on the relevance of our results to the broader vascular malformation in the Discussion section in Lines 374 to 386 as follows:

*"Our unique perspective on the mechanics of the heterogenous vascular tissue during lesion growth opens up a complementary avenue for further in-vivo exploration. Owing to the shared mechanisms, studies on CCM pathogenesis have proven exceptionally valuable in shedding light on vascular development and other diseases. SWS is one such low flow vascular malformation (VM) which is also associated with increased EC migration through the activation of RhoA and Rac1 signaling, and a low mutation frequency in affected tissues*15,19*. Mutations associated with high flow malformations, such as those in HHT, can also lead to vascular overgrowth, high migratory and invasive behaviors and increased sensitivity to proangiogenic cues from an overactivation of PI3K signaling*16,17*. On the other hand, PI3K-driven VMs in mice require active angiogenesis for the pathogenesis of malformations*18*. Lymphatic malformations associated with mutations in PIK3CA result in hypersprouting, but only a fraction of lymphatic ECs carry the mutation. One suggested possibility is that the small population of mutant clones use clonal cooperation to signal to normal ECs in the neighboring regions leading to their potential functional alterations*75*. As such, our findings here could also offer a novel mechanics-driven model for lesion growth in these other conditions seeded by somatic mutations and presenting mosaic lesions."*

Minor Comments:

1. **For multiple comparisons, Dunn's correction is used instead of Dunnett. Dunnett is more commonly used when comparing to a control group, whereas Dunn is more commonly used for multiple comparisons with no clear control. How do p-values hold up with Dunnett correction? And if using Dunn correction, please include table with statistics for all comparisons (siCCM2 vs ROCK1 and ROCK2, ROCK1 vs ROCK2 etc) to better understanding the statistical findings.**

When choosing a statistical method, we first checked if the dataset fit normality/a gaussian distribution. We found that while some of the conditions did have a normal distribution, not all conditions satisfied this criteria. Since it would be inappropriate to use a parametric statistical test to compare conditions that do not all show normality, we chose a non-parametric Kruskal Wallis test with Dunn's correction for multiple comparisons. When applying a one-way ANOVA test with multiple comparisons for normally distributed data, we can use a Dunnett's correction which has a higher statistical power. We have tested this and found no difference in the conclusion. We have now included a "Source Data" excel spreadsheet with the raw data along with the statistical comparison tables for each quantification presented in figures in the paper.

P-values comparing statistical methods for strain energies computed in Table 3

Comparisons	Kruskal Wallis with Dunn's	ANOVA with Dunnett's
siCT vs *siCCM2*	0.0006 (***)	0.0043 (**)
siCT vs *siCCM2+ROCK1*	>0.9999 (ns)	0.9763 (ns)
siCT vs *siCCM2+ROCK2*	>0.9999 (ns)	0.7254 (ns)
siCCM2 vs *siCCM2+ROCK1*	0.0013 (**)	-
siCCM2 vs *siCCM2+ROCK2*	<0.0001 (****)	-
siCCM2+ROCK1 vs *siCCM2+ROCK2*	>0.9999 (ns)	-

2. **Authors suggest a transcriptomic transition to a "stalk-like identity", is a stalk-like identity defined transcriptomically in the existing literature. Is there a set of canonical markers previously shown to be enriched in endothelial cells that behave as stalks? Otherwise it is not clear that the transcriptomic changes are not incidental in regards to the stalk identity.**

Indeed, stalk cell markers have previously been identified in various studies. We have now added two such genesets corresponding to stalk cell markers identified from two sources: (i) tumor endothelial cells and, (ii) normal endothelial cells during sprouting angiogenesis. We found that wild-type ECs from mutant mosaics (WT-CCM2) presented a signature of stalk cells in a tumor context, but not that of a normal endothelial sprouting context. We have added these genesets to the dotplot presented in Fig. 4h.

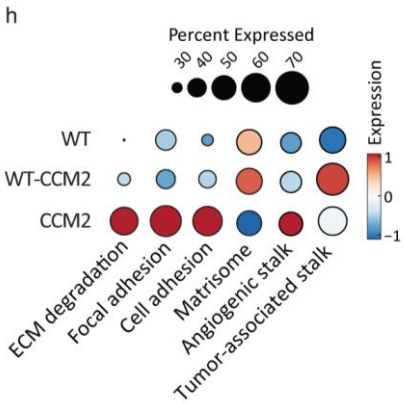

Fig. 4: h. Dotplot representation of ECM degradation, focal adhesion, cell adhesion, matrisome, angiogenic stalk ECs and tumor-associated stalk ECs signaling pathways compared across the dataset.

Further, we have now adapted the text in Lines 293-296 as follows :

> *"In contrast, WT-CCM2s presented a stalk cell signature associated with tumor endothelial cells but not normal endothelial cells, suggesting that WT-ECs behave as pathological stalk cells in a CCM environment (Fig. 4h)*56,57*. These predominantly stalk WT-CCM2s further presented upregulated genes linked to ECM deposition termed "matrisome" (Fig. 4h, Supplementary file 4)."*

3. **For the transcriptomic analyses, are the siCCM2 cells generated from mosaics as well or are those monolayer siCCM2 cells?**

We first allowed mosaics of silenced and wild-type cells invade the matrix as was the case in the previous presented results. For the transcriptomic analysis, we then removed and dissolved the hydrogels in trypsin to collect the mosaic population of invaded cells (Fig. 4a) . We did not use trypsin in the dish itself to only collect cells bound to the hydrogel that was removed from the dish. The mosaic cells were then FACS sorted to collect siCCM2 (or siCT) and WT cells from each hydrogel (Fig. 4a). All cells from the transcriptomic analysis were collected post-angiogenic invasion of mosaics cell populations and must have been adhered to the hydrogel.

4. **%Edu positive cells in figure 4, is that determined by single cell transcriptomic data? It appears to be inconsistent with the staining quantification after 48 hours in extended data 6. Please**

explain how these figures correspond to each other and include such a discussion in the main manuscript to clarify the finding.

The % of EdU positive cells quantified in Fig. 4 is determined by using the EdU staining kit on 1:1 2D mosaic cell populations cultured in plates for 48h. The same system was used for the quantification presented in Extended Data Fig. 6. However, Extended Data Fig. 6 presents a control experiment used to compare the % of EdU positive cells between 24h and 48h of culturing. It represents data from one trial and has a smaller dataset. Since we observed that 24h was too short for changes in EdU based on this control experiment, we performed the remaining experiments at the 48h timepoint. This data is presented in Fig. 4 and includes 3 independent trials. The differences seen are a result of the larger (and complete) dataset presented in Fig. 4. This has also been previously described in the results section of the manuscript text in Lines 302 to 308 as follows:

> *"To validate this finding, we first checked for EdU-positive WT nuclei in CT or CCM2 mutant mosaics after 24h of invasion and observed no differences. We then explored this in 2D by comparing EdU-positive WT nuclei from a 1:1 mosaic with siCCM2 versus siCT ECs cultured for 24h or 48h. Notably, we observed a significant increase in EdU positive WT nuclei in CCM2 mutant compared to CT mosaics after 48h in 2D (Fig. 4k), but saw no clear differences at the 24h timepoint (Extended Data Fig. 6-A). This suggested that our 24h sprouting assay may have limitations in exploring this mechanism through staining in the 3D context, despite the upregulation of DNA replication genes observed by single cell RNA sequencing."*

Reviewer #2 (Remarks to the Author):

The manuscript, entitled "Force-mediated recruitment and reprogramming of healthy endothelial cells drive vascular lesion growth" by Shapeti et al., investigates mechanical mechanisms underlying a vascular abnormality, CCM, using HUVEC 3D cell culture, 3D TFM, and single-cell sequencing. First, the authors examine 3D angiogenic sprouting of the HUVEC in PEG hydrogel, finding that loss of CCM2 enhances angiogenic sprouting potentially through elevated cell-ECM forces and hydrogel matrix degradation via ROCK signaling pathways. Then, they explore the influence of CCM2-silenced ECs on surrounding wild-type ECs and found that WT ECs' invasion modes into the hydrogel are changed by CCM2-silenced ECs and ROCKs. Following that, they investigate the potential mechanisms of this change and claim that hyperactive CCM2-silenced ECs influence WT ECs by potential residual ECM components, pulling forces, and reinforcement of WT EC actin cytoskeleton. Furthermore, the manuscript uses single-cell RNA sequencing to show that CCM2-silenced cells reprogram recruited WT ECs into a proliferative stalk cell identity, indicating a potential mechanically-driven cell reprogramming.

Mechanics has proven vital in various biological processes such as morphogenesis and angiogenesis, as well as in the pathogenesis of diseases like cancer and cardiovascular diseases. Yet, the exploration of mechanics in vascular diseases, particularly within cerebral systems, remains limited. This work delves into a compelling topic by investigating the mechanical mechanisms involved in vascular diseases, offering potential insights into the role of mechanics in tissue heterogeneity and disease progression. This research has the potential to gain significant attention from the field. However, some of the conclusions do not yet appear to be justified by the data. Therefore, we offer the following comments that should be addressed.

Major Comments:

Overall, the manuscript needs improvements to draw its conclusions because of the following concerns.

1. **The manuscript lacks clarity in the description of the 3D models used, limiting the potential for reproducibility. The authors use schematics to describe their experiment setups, such as Figs. 1a, 2a, 3a etc., but there is no single image showing the real setups. Providing a clear depiction of experimental setups, including details such as device images, hydrogel thickness, and a 3D schematic of the device with scale bars, would enhance the transparency and replicability of the study. Moreover, in reference 59 where the authors describe their model, it is somewhat unclear whether the sprouts are extending on top of the gel or penetrating into it. Fig. 1a,b in that paper appear to show sprouts on top of the gel.**

   We thank the reviewer for this important comment. Indeed we only included the schematic since we had previously published work using a similar model [12,30]. This comment brought to light the importance of emphasizing the specifications of our model in the first figure to ensure clarity for the reader. We have now included an image of a well with the actual chamber attached, a 3D representation of the system and the associated dimensions. We have also included an image of the overall invading monolayer for emphasizing the early steps of angiogenic sprouting that we capture as well as a 3D render. All results presented in this paper are associated with 3D sprouts penetrating into the hydrogel and not extending only on top of the gel. To also aid application of this system for future studies by the scientific community, we are currently preparing a follow-up protocols manuscript with detailed recommendations to replicate this model. The newly added figures are shown here below:

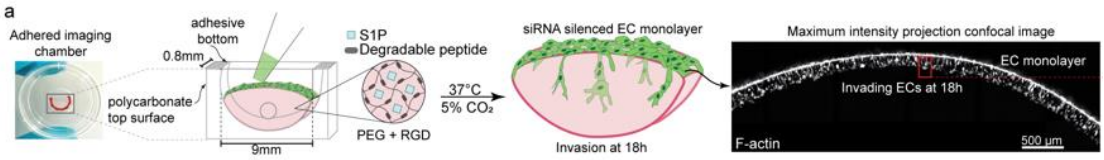

Fig. 1: a. Schematic representation of the PEG hydrogel based 3D angiogenic invasion assay.

2. **In the present paper, the authors have changed from using collagen to a functionalized PEG gel. This differs from true extracellular matrix in several important aspects: 1) The mesh spacing in a PEG gel is much smaller than in collagen, for example. Hence the sprouting (assuming it penetrates the gel) requires matrix degradation to occur whereas in other, perhaps more physiological gels, the interfiber spacing could be sufficiently large to allow filipodia to extend without degradation. 2) Also due to the small mesh spacing, diffusion of signaling molecules could be impeded relative to in vivo. This might accentuate the effects of mechanical signaling due to suppression of biochemical signaling. 3) While real ECM would be degraded by a wide range of MMPs, the PEG gel used here appears to have just one MMP-cleavable linkage. Thus, statements regarding the role of a single integrin or MMP may not be generalizable.**

   All this leads to the point that the authors need to provide a deeper discussion of their choice of gel and the potential artifacts associated with it. Their results specifically pertain to a gel with particular cleavage and adhesion proteins tethered to the matrix.

   We thank the reviewer for this reflection on the validity of our model ECM. The vascular basement membrane in the healthy brain is normally composed of Collagen IV, laminins and proteoglycans, whereas the pathological brain is associated with fibronectin [31]. Since the brain extracellular matrix does not normally contain Collagen I (as typically used for collagen gels), we chose to move to a different hydrogel system. Brain capillary endothelial cells, pericytes and astrocytes are all known to bind to Collagen IV in the vascular basement membrane through β1-integrin [31]. RGD motifs are present on both Collagen IV and fibronectin, and are known to interact with β1-integrins (and most other β integrins as well) [32,33]. Importantly, increased β1-integrin signaling is also proven to be crucial for the CCM phenotype [34,35]. This was the rationale for choosing an RGD-conjugated hydrogel system.

   Further, matrix degradation is known to be important for CCM lesion formation. Blocking ADAMTS4 proteases in mice is shown to reduce CCM lesion formation in neonatal mice [36]. As a result, we chose a system where degradation is important for invasion. Using a non-degradable PEG hydrogel blocked invasion showing that degradation was necessary to invade the PEG matrix (Extended Data Fig. 2B). Subsequently, we chose PEG hydrogels conjugated with a GPQGIWGQ MMP-cleavable peptide sequence. This sequence is cleavable by multiple MMPs, namely 1, 2, 3, 8 and 9 [37]. Pathological areas in resected human CCM lesions have recently been shown to overexpress MMP2 and MMP9 [38,39]. Since our peptide is cleavable by both, we expect to capture this effect. We would also like to emphasize that invading cancer cells have been shown to create degraded tracks even in Collagen I hydrogels [40]. Consistently, blocking MMP-dependent degradation is shown to reduce endothelial sprout width in Collagen I hydrogels, suggesting that degradation is an important mechanism in collagen-based hydrogel systems as well [41].

While our hydrogel should sufficiently activate relevant integrins and degrade in response to key MMPs implicated in CCM pathogenesis, it is nevertheless a confined, nanoporous synthetic network. This might be different from the in-vivo environment, both in terms of the porosity and fibrillarity. The exact properties of the modified in-vivo ECM associated with CCMs remains to be characterized. CCM mutant ECs are, nevertheless, shown to aberrantly remodel their extracellular matrix by depositing both fibronectin and collagen I [35]. Our transcriptomic analysis on WT ECs from mutant mosaics that have invaded the PEG matrix shows that they express matrix deposition proteins, which is likely to help them create a perivascular environment more similar to the in-vivo situation. Our PEG hydrogels were previously determined to have an average pore diameter of 25 nm [42]. Since the hydrodynamic radius of common angiogenic factors such as FGF-2 and VEGF is not larger than 3 nm, we do not expect the pore size to have any considerable effects on protein diffusion through the PEG hydrogel matrix [43].

While we agree with Reviewer 2 that the structure of our hydrogels does not exactly mimic the in-vivo extracellular matrix, an RGD-conjugated, degradable PEG network could nevertheless provide a sufficient reductionist model for studying CCM pathological angiogenesis. We acknowledge that despite our best efforts at choosing an appropriate ECM-like network, our results are specific to this system and would require in-vivo studies to confirm similar effects. To this end, we have included a description of this caveat in the discussion. This can be found in Lines 325-331 as follows:

> "*One limitation to our study is that our synthetic, nanoporous hydrogel does not perfectly mimic the microporous structure of the in-vivo ECM so that our findings might be specific to its biochemical composition.. However, in order to make it suitable for cell adhesion, the hydrogel was conjugated with RGD peptide which is found in both fibronectin and collagen IV, and interacts with β1 integrins that are overactivated in CCMs*49,63*. Further an MMP-cleavable peptide was also included which is degradable by MMP2 and MMP9 – both shown to be overexpressed at CCM lesion boundaries*40,41,64*. We believe this model even though reductionist provides important clues driving invasive behaviors."*

3. The manuscript lacks validation through raw 3D images. For example, validation of the claims of this manuscript depends on their relevant 3D network structures, but there are no 3D images (e.g., confocal imaging) to confirm that, such as how thick are the networks, what are the dimensions of the lumens if they exist, etc. Another example is that they only showed local mosaic images, without any sprouting network images in one big device, making it difficult to a certain the influence of how they select the samples on the final analysis of the results.

We thank the reviewer for suggesting that we provide 3D renders to validate the 3D nature of our sprouting. We have now added a looped video with a visualization of the 3D structure of sprouts (Supplementary Video 1A). We have also added a 3D reconstruction of a sprout with an XYZ plane representation in Figure 1a as shown below. This combined with the new details added to the schematic of our model in Fig. 1a should better explain the nature of sprouting observed in our system.

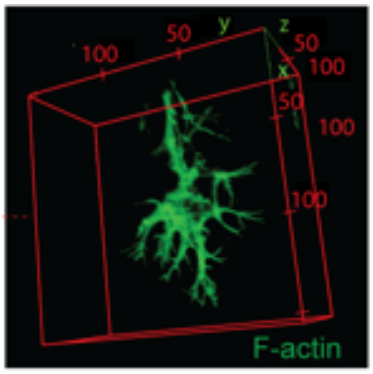

We would like to clarify that every sprouting image presented in this study is obtained by 3D confocal imaging with a z-stack thickness ranging between 40-100 µm, dictated by the thickness of the sprout of interest. This is also a prerequisite for reliable data acquisition for 3D traction force microscopy. The representative figures in the manuscript as well as the videos are all maximum intensity z-projections of 3D confocal image stacks. Fig. 2k further shows the sectioning of a 3D CCM2 mosaic sprout to highlight contact between the WT ECs and siCCM2 ECs in the z-plane.

Additionally, as is shown in the updated Fig. 1a, our model consists of an adhesive imaging chamber attached to a glass bottomed culture dish to provide a semi-confined framework to form the hydrogel consisting of a uniformly distributed proangiogenic cue. ECs first form a monolayer by attaching to this hydrogel interface, followed by invading the hydrogel upon angiogenic activation due to the proangiogenic cue. This assay is different from a more complex, longer-term microfluidic device with a stable angiogenic gradient allowing for long term vessel formation. Our model can only sustain early angiogenic invasion for up to 24 hours. The results presented in this manuscript are at between 16-20h of invasion. Overnight timelapse imaging shows the evolution of sprouting from 0h post cell seeding up to 16h, as is visible in Supplementary Videos 2A-D. Given the short term nature of our assay, we do not capture extensive stable vessel networks or lumen formation, as is the case in microfluidic devices. We do, however, capture the early cell-cell and cell-ECM interactions that initiate angiogenic sprouting.

An example of overall sprouting in our imaging chambers is presented in Extended Data Fig. 1. We did not include further images or characterizations of overall sprouting because we already presented this in our previously published study which primarily compared the invasive capacities of siCT versus siCCM2 in both mosaic and non-mosaic systems [7]. Since our focus in the current manuscript was to extend this initial work to identify more detailed mechanisms at the cellular level, we highlight the morphology at the cellular level where these mechanisms occur. The selection of the samples for the final analysis was done by taking multiple positions starting from one end of the monolayer to the other at consistent intervals to ensure that we capture the behavior of this entire global invasion. Further, at least 10 positions were captured for every given monolayer (1 entire chamber or sample) to ensure that we appropriately captured the local as well as global behavior of the sprouting without bias. This was repeated for 2-3 independent experiments, unless otherwise mentioned. These aspects of experimental design were detailed in the Reporting Summary submitted alongside the manuscript. We have now also added a description directly in the statistical analysis section of the methods as follows in lines 872 to 877:

> "*Measurements were taken from several distinct cell sprouts within a sample and the same cell sprout was repeatedly measured only for overnight imaging to study the dynamics. The selection of sprouts was done by taking multiple positions starting from one end of the monolayer to the other at consistent intervals to ensure that we capture the behavior of this*

entire global invasion. Further, at least 10 positions were captured for every given monolayer (1 entire chamber or sample) to ensure that we appropriately captured the local as well as global behavior of the sprouting without bias. Additional aspects of experimental design are detailed in the Reporting Summary."

4. **The manuscript lacks percentage comparison details. The manuscript relies on percentage comparisons without providing the necessary context such as absolute numbers, variations among cells, etc. Examples are:**
    a. **In Result 3, "Remarkably, we observed that 80% of invading WT ECs in CCM2 mutant mosaics…". This statement lacks context without absolute numbers of cells in each mode. It's crucial to present these numbers to fully understand the percentage comparisons here. For instance, in Fig. 2g, the 0% of invading WT ECs classified as Mosaic Stalkers in CT mosaics can be misleading since there are no CCM2-silenced cells in this group, resulting in a total count of zero. A comparison between groups like CCM2 and CCM2-ROCK1 also necessitates the inclusion of absolute numbers for a valid comparison.**
    b. **In Result 4, "Strikingly, WT ECs in mutant mosaics regain tip cell behavior when either ROCK1 or ROCK2 is depleted in the siCCM2 EC". The total numbers of cells exhibiting this behavior need to be provided to substantiate this claim.**
    c. **In Result 5, "Taken together, this establishes that CCM2 loss drives a ROCKs-dependent non-autonomous inhibition of leader cell behavior in WT ECs". The total numbers of cells exhibiting this behavior need to be provided to substantiate this claim.**

We first adapted the text as follows in Lines 158 to 161 to clarify the compositions of the two mosaics situations:

"To further explore angiogenic activation of WT ECs by CCM mutants, we visualized collective sprouting in two situations: (i) CT mosaics where LifeAct-RFP tagged WT ECs were mixed with LifeAct-GFP tagged siCT ECs, and (ii) CCM2 mosaics where LifeAct-RFP tagged WT ECs were mixed with LifeAct-GFP tagged siCCM2 ECs in various percentages."

In response to comments a, b and c, we have now added a supplementary table with the raw absolute numbers of WT ECs quantified in each mode of invasion. Such a table was also required by the journal to show the raw data for each figure. Therefore the details requested here are included in a sheet associated with the figure number, in this case Fig. 2j. A summary of this table is also included here:

Invading WT ECs	TOTAL	Lone tip	Mosaic stalk	Trailing tip	Mosaic tip
CT mosaics	18	17	0	0	1
CCM2 mosaics	41	3	34	4	0
CCM2+R1 mosaics	27	24	2	1	0
CCM2+R2 mosaics	39	14	17	6	2

Additionally, we have also modified the labeling in the Fig. 2i as well as the caption of Figure 2i, j to include the total number of WT ECs counted for each of the conditions as follows:

"Figure 2: ***i.*** *Schematic representation of categories of wild-type ECs defined based on their position relative to silenced ECs (siCT or siCCM2 in the respective mosaics) at the start of ECM invasion.* ***j.*** *Quantification of the percent categorical distribution of the various modes of invasion described (in i) for WT ECs in CT versus CCM2 mutant mosaics. The total number of invading WT ECs counted for each condition are: CT mosaic=18 , CCM2 mosaic=41, CCM2+ROCK1 mosaic=27 , CCM2+ROCK2 mosaic=39 (3 independent trials with 3 FOVs/trial containing between 15-20 cells each per condition)"*

To further clarify, the quantification of the various modes of invasion of the WT ECs were performed as follows:

We first defined the four categories of invasion as represented in the schematic in Fig. 2i. For each mosaic condition (ie. CT mosaic, CCM2 mosaic, CCM2+ROCK1 mosaic, CCM2+ROCK2 mosaic), we manually counted the number of WT ECs from a given mosaic condition in each mode at the first moment of invading the hydrogel as visualized in overnight timelapses. Based on this, we were able to compute the relative number of WT ECs invading in each mode for each condition. It is indeed true that this percentage does not also give an overview of how many total WT ECs were captured invading in each condition, which is now explicitly mentioned in the captions as well. We thank the reviewer for pointing this out.

5. **Please clarify Sample Numbers (n). The meaning of sample size (n) is unclear. Is it device numbers or cell numbers? If cell numbers are used for comparison, further evidence of small variations among devices and overview images of sprouts are needed.**

Here below we discuss the design of our experiments and the rationale:

Sample size: Experiments were conducted with a minimum of two independent trials and multiple biological replicates. Sample numbers (n) is the total number of cells captured from the multiple independent trials. In each legend we mention the number of independent trials as well as the total number of data points (n). For scRNAseq, we pooled cells from four independent trials and three technical replicates.

For all other experiments in PEG hydrogels after angiogenic invasion, one dish with an endothelial monolayer of HUVECs invading the gel in a chamber was considered one independent trial when performed in independently prepared gels and independently prepared cells. Each experiment consisted of one well per condition, a newly thawed batch of ECs and an independent set of transfections on this batch of EC. This captured the variability from the cell source, transfection protocols and hydrogel preparation.

Multiple biological replicates, which refers to at least 10 data points selected over the range of the entire monolayer, further captured the variability within a single chamber. These replicates captured the variability within a given hydrogel from various sources: the inherent biological variability of the invading endothelial cells, the dynamic nature of cellular force exertion, and any topography effects on location specific invasion. We relied on our previous experience to determine these sample sizes which we deemed sufficient as they accounted for the variability inherent to pooled HUVECs and led to reproducible results. Our sample size was large enough to capture differences between conditions of siRNA transfected cells as well as wild-type cells.

Randomization: The culture and siRNA transfection conditions, PEG invasion assay preparation times, 3D TFM imaging times and overnight imaging times were kept constant to eliminate sample-specific characteristics that can impose variations in our data - this allowed us to reliably interpret the results and attribute them to the specific cell treatment. For selecting replicates within a given endothelial monolayer invading a given hydrogel, we imaged 10 randomly chosen locations from left to right of the monolayer ensuring a sample from each curvature of the monolayer to limit any location dependent effects.

Each datapoint in Fig. 2b represents one independent experiment (for one entire chamber), where we compare the global invasion distance of WT ECs in the entire monolayer between siCT and

siCCM2 mosaic conditions. The 50-50% bar of this graph shows the variation within the devices, which we have also shown in our previously published study using the same conditions, protocols and chambers [7].

6. **The claim that CCM2-silenced ECs lead 80% of WT ECs as "mosaic stalkers" lacks validity. The authors did not investigate whether the CCM2 ECs also induce changes in other CCM2 ECs. The observed alterations may stem solely from the adherence of wild-type (WT) ECs to the CCM2 ECs, potentially indicating a passive influence (that the CCM2 ECs are simply dragging the WT ECs along) rather than a positive regulatory effect. Further elucidation is required to provide a more comprehensive understanding of this phenomenon.**

   As explained in Major Comment 4, we quantified the WT EC categories as follows:

   After defining the four categories of invasion presented in the schematic in Fig. 2i, we counted the number of WT ECs in CCM2 mosaics that begin invading the hydrogel as “mosaic stalks”. We also counted the total number of WT ECs that invade the hydrogel in CCM2 mosaics, and assign them one of the four defined categories. This gave us the percentage of invading WT ECs which were in mosaic stalk positions, which we found to be 80% in CCM2 mosaics. Similarly, when computing this for siCT mosaics, we counted how many of the total invading WT ECs were in mosaic stalk positions and found this to never occur.

   Further, our cell-ECM and cell-cell force quantifications together showed that WT ECs in stalk cell position rarely exert forces on the ECM themselves but feel pulling forces from the highly contractile leading CCM2 tip ECs. As a result, we indeed proposed that mutant cell force exertion is contributing to WT stalk cell forward motion, as if mutant cells are capable of physically “dragging” WT cells forward. While this may seem as WT ECs that passively undergo force exertion from mutant cells for their migratory behavior, we also demonstrated regulatory effects in terms of phenotypic changes and reprogramming of WT cells in mutant environments, as evidenced by immunofluorescence (increase in β1-integrin focal adhesions, reinforcement of the actin cytoskeleton) and single cell RNA sequencing. Together, it suggests the exciting possibility of force-induced changes in WT cell identity, such as upregulation of proliferation and stalk-cell identity (Fig. 4h-k). It is possible that CCM2 ECs also affect other CCM2 ECs. However, our goal was to understand the effects of CCM2 mutant ECs on neighboring normal ECs and propose a mechanism for lesion growth as the symptomatic human lesions are >80% enriched with normal WT ECs. Consistently, we also saw an enrichment of WT ECs with time in these mosaic invading cultures (described in more detail in response to the next comment), suggesting the importance of WT EC contribution.

7. **The manuscript lacks proof of the WT EC contribution. The manuscript lacks evidence proving the contribution of WT ECs to true multi-cellular angiogenic sprouting as opposed to 1-2 cell migration/protrusion, limiting the impact of the work. Longer-term cell cultures might be used to prove the impact of WT ECs on angiogenesis.**

   We thank the reviewer for this comment. It is certainly true that our short term angiogenic sprouting model is limited in capturing how these observed effects on WT EC behavior impact longer-term stable vessel formation. Such a model is currently being developed in our group as a follow-up to this work.

Nevertheless, to illustrate that the mosaic cultures became more enriched for wild-type ECs over time, we added two additional quantifications to Figure 2 based on the 18h overnight films. We were unable to timelapse image nuclei using Hoechst because of phototoxicity from the UV in large 3D stacks. To circumvent this, we chose to quantify the area occupied by each cell type over time as a substitute for cell numbers (**Error! Reference source not found.**). In addition, we also represented this as relative percentages of area covered by siCCM2 mutants and wild-type ECs as a measure of their relative enrichment with time (**Error! Reference source not found.**). Further, we also quantified the number of mutant versus WT nuclei in mosaic sprouts observed after 18h of invasion (**Error! Reference source not found.**). This gives an estimate of the number of WT nuclei that followed behind leading siCCM2 ECs.

Based on these new quantifications, we found that both siCCM2 and WT ECs were enriched with time in the gels, as seen in the area occupied by them in **Error! Reference source not found.**. Consistent with the previously quantified invasion distance over time, WT ECs are delayed in invading the matrix confirming that the mutant ECs have an invasive advantage. After this initial delay, WT ECs begin to progressively occupy more area of the matrix. Moreover, there is an increase in the percentage of area occupied by WT versus siCCM2 ECs with time as shown in **Error! Reference source not found.**, showing that WTs get enriched once the highly invasive mutant tips have migrated forward. Finally, when looking at the mosaic sprouts at the end of the experiment after 18h, we saw a ratio of 1 CCM mutant for 3 WT ECs (**Error! Reference source not found.**).

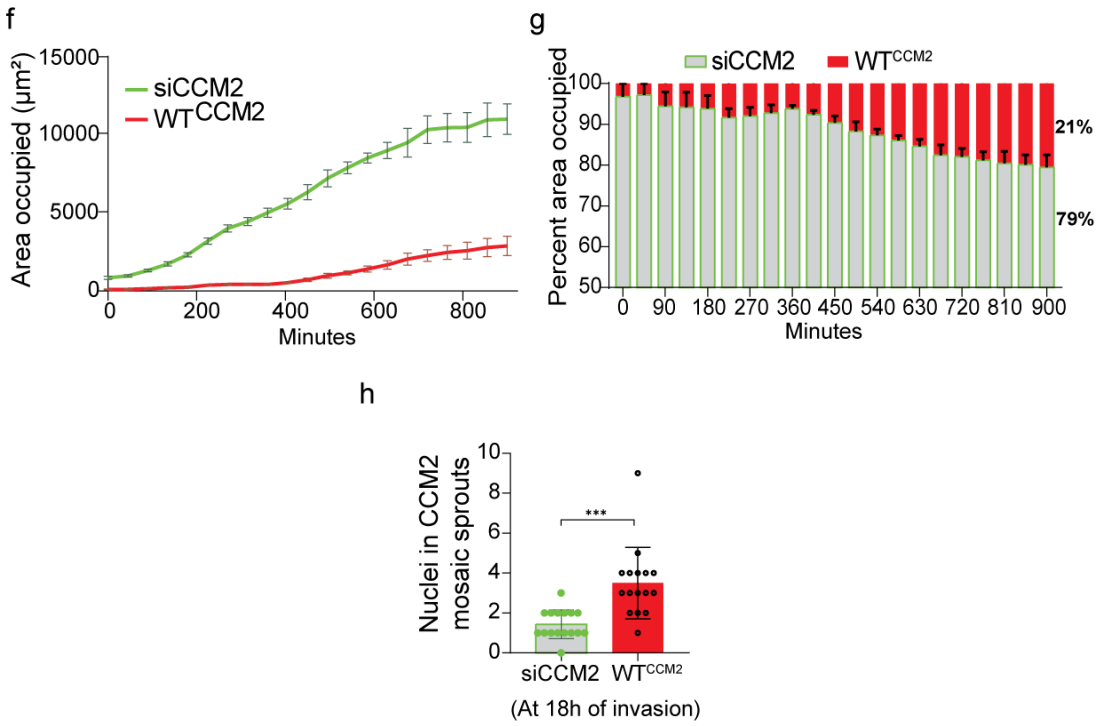

Fig. 2: **f.** Automated quantification of the progressive area of the matrix occupied by each cell type in CCM2 mutant mosaics. **g.** Relative matrix area occupied by each WT or siCCM2 ECs in CCM2 mosaics showing WT enrichment over time. **h.** Number of nuclei quantified in mosaic sprouts composed of WT and siCCM2 ECs after 18h of invasion in CCM2 mutant mosaics. 2 independent trials with a total of 16 mosaic sprouts compared using a Wilcoxon test.

We also adapted the text to include these new quantifications in Lines 171 to 181 as follows:

"Tracking dynamics of angiogenic sprouting over 18h showed that both siCCM2 and WT ECs begin invading earlier and faster in CCM2 mutant mosaics than in CT mosaics (Fig. 2c-e,

Supplementary Videos 2A-B). However, siCCM2 ECs initiated invasion earlier than the WT ECs in these CCM2 mutant mosaics and had an invasive advantage as shown by their increased invasion speed (Fig. 2d,e). Further, we saw an enrichment of both siCCM2 and WT ECs with time in the gels, as seen with the matrix area occupied by them in Fig. 2f. Consistent with Fig. 2c, WT ECs are delayed in invading the matrix confirming the invasive advantage of mutant ECs. After this initial delay, WT ECs began to progressively occupy more area of the matrix. Moreover, there was an increase in the relative area occupied by WT versus siCCM2 ECs with time (Fig. 2g), showing that WTs got enriched once the highly invasive mutant tips had migrated forward. Finally, when looking at mosaic sprouts at the end of the experiment after 18h, we saw a ratio of 1 CCM mutant for every 3 WT ECs (Fig. 2h). This was consistent with in vitro findings where CCM spheroids got enriched with WT ECs from neighboring monolayers[3]*"*

8. **The Supplementary Text, especially the equations, has somehow been distorted in the file we received, so it would be helpful to receive another version of that.**

   We have uploaded a new version of the supplementary document. We have also additionally included a separate pdf file titled "Supplementary Notes" with only Supplementary Note 1 and 2 so the equations are maintained and visible.

Minor Comments:

1. **In the abstract, the phrase "Here, we use 3D traction..." should be revised to "Here, we utilize an in-vitro model involving 3D traction..."**

   We have modified this sentence in the abstract as follows:

   "Here, we utilize an in-vitro model of early angiogenic invasion involving traction force microscopy to reveal that hyper-angiogenic CCM2-silenced endothelial cells enhance angiogenic invasion of neighboring wild-type cells through force and extracellular matrix-guided mechanisms."

2. **In Fig 1, it is necessary to provide a rationale for the significantly higher variations observed in the siCCM2 groups compared to other groups.**

COEFFICIENT OF VARIATION

	siCT	siCCM2	siCCM2+siROCK1	siCCM2+siROCK2
DISPLACEMENTS	0,47	0,34	0,40	0,43
TRACTIONS	0,38	0,33	0,35	0,44
ACTIN INTENSITY	0,62	0,55	0,68	0,53
NUM FILOPODIA	0,91	0,62	0,55	0,62
FILOPODIA LENGTH	0,64	0,32	0,50	0,42

We calculated the coefficient of variation, which is a statistical measure of the dispersion of data points around the mean, for various metrics quantified in Fig. 1. We surprisingly found that the variations in siCCM2 are consistently lower than those observed in siCT suggesting the strong phenotype of these mutant cells.

3. **In Fig. 1b, while only the first and third images currently depict the monolayer morphology, it would be beneficial to include monolayer representations for the second and fourth images for consistency and clarity. This suggestion applies similarly to Figure 3b.**

   We thank the reviewer for this comment. In order to sufficiently resolve the filopodia and sprout tip morphologies in Fig. 1b and to resolve bead displacements in Fig. 3b, it was necessary to acquire images at a high magnification and resolution. Since the invasion in siCCM2 and siCCM2+siROCK2 groups was significantly higher compared to siCT and siCT+siROCK1, the sprout tips had migrated much farther away from the monolayer. Since it was crucial that we took images at the same resolution to quantitatively compare the groups, this invasive difference made it impossible to also capture the monolayer in the same field of view for the highly invasive siCCM2 and siCCM2+siROCK2 conditions. The lower magnification images comparing invasion in our previously published work, nevertheless, capture the monolayers for both mosaic and non-mosaic sprouting for all the conditions[7].

4. **The absence of overview images in the paper, particularly where percentages are used to substantiate claims (such as in Figure 2g), is a limitation. Without comparing the entire structures across different groups, relying solely on percentage comparisons may lead to misinterpretations or incomplete conclusions.**

   Our previous work published in 2021 [7] already included overall invasion images and quantifications for both mosaic and non-mosaic sprouting in siCT, siCCM2, siCCM2+ROCK1 and siCCM2+ROCK2 conditions. However, for the sake of clarity, we have now added an overview image of the invasion alongside the more detailed schematic of the system used in Fig. 1a. Since the focus of our present work was to study more detailed mechanisms leading to this overall invasive behavior observed in our previously published study [7], we highlight the morphology at the cellular level where these mechanisms occur as opposed to the global level. As described in the response to Major Comment 5, we take multiple positions starting from one end of the monolayer to the other at consistent intervals to ensure that we capture the behavior of this entire global invasion. The datapoints from one independent trial correspond to each of these positions. Further, as described in Major Comment 4, we now also included the absolute sample numbers of each of the groups in addition to the percentages, and further provide the raw numbers in the "Source Data" to allow for a more comprehensive understanding of our data.

5. **In Result 1, the discussion around Rho-associated coiled-coil forming protein kinases (ROCKs) requires a more detailed explanation, especially for readers who may not be familiar with this topic. Clarifying why ROCKs were specifically chosen for this study would make the results more accessible to a broader audience.**

   We have now adapted the text to include a description about ROCKs before introducing our results associated with ROCK1/2 silencing as follows in Lines 97 to 100:

   "ROCKs are direct effectors of RhoA known to regulate the morphology of the actomyosin cytoskeleton in 2D monolayers[44]. In particular, in CCM mutant ECs we previously showed that ROCK1 mediates integrin-anchored actin stress fibers while ROCK2 promotes cortical actin polymerization[45,46]. In 3D, we saw that ROCK1 but not ROCK2 mediates the increased invasive capacities of CCM2 silenced ECs[7,45]."

6. **In Result 2, "Surprisingly, the numerous filopodia still observed in siCCM2+siROCK2 sprouts did not translate to higher forces on the ECM (Fig 1d,e)." The role of myosin II and its relationship with ROCK in force generation should be also considered. Highlighting that more actin doesn't necessarily equate to higher forces could clarify why this observation might not be as surprising.**

   We have now adapted the text to discuss this aspect in more detail in Lines 117 to 125 as follows:

   "This was consistent with the decrease in filopodia upon ROCK1 depletion, as previously observed in dendritic cells where ROCK1 was necessary for Rac1-dependent filopodia at the front (Fig. 1d,f) [17]*. Taken together, this suggests that tractions exerted by siCCM2 ECs were associated with the abundant ROCK1-dependent tip cell filopodia. Surprisingly, the highly invasive siCCM2+siROCK2 sprouts with their numerous filopodia did not generate higher forces on the ECM (Fig 1d,e), suggesting a lack of myosin II-dependent contractility. Interestingly, ROCK2 was previously reported to generate contractile force at filopodia through the phosphorylation of myosin-light chain and cofilin in dendritic spines* [17]*. Consistently, we found that ROCK2 silencing had a stronger effect on rescuing forces than ROCK1 at the numerous ROCK1-dependent filopodia, as is visible in the lower displacements, tractions and strain energies."*

7. **In Result 2, more explanation of MT1-MMP is needed for a broader audience.**

   Thank you for the comment. We have now added a brief context to MT1-MMP in the results from Lines 131 to 135 as follows:

   *"MT1-MMP is a transmembrane metalloprotease which localizes to focal adhesion sites and activates MMP2 and MMP9, both of which are overexpressed in CCM lesions*40–42*. Further, MT1-MMP-dependent ECM degradation is known to drive cancer cell invasion and angiogenesis*43,44*. Immunostaining for MT1-MMP, also confirmed an increase in MMP expression, especially at the rear of the cell (Fig. 1k,l)."*

8. **In Result 5, the statement "When observing invasion dynamics, we often noted that hyper-migratory siCCM2 tip cells…" requires quantification of the term "often." Additionally, providing a histogram or similar graphical representation in relation to Figure 3g would substantiate the claim with concrete data.**

   We were interested in the first part of the process which is the mechanical pulling of WT ECs by mutant ECs, a process that we have carefully described and quantified over the different figures. The mention to the retraction upon detachment is only to further evidence the mechanical dragging of the WT ECs, as it is most likely the consequence of the relaxation of its acto-myosin cytoskeleton maintained under tension through the cell-cell contact with the mutant cell (increased actin and β1 integrins as a proof of this). Nevertheless, we analyzed timelapse videos taken in 9 fields of views from 3 independent trials and identified a total of 26 mosaic sprouting cases where a CCM2 mutant tip EC leading a stalk WT EC eventually detaches and migrates away, leaving the stalk WT EC behind. The frequency of this detachment could not be correctly quantified because the angiogenic invasion process in our model is highly dynamic wherein cells leave the monolayer to begin invading the matrix at different timepoints. Since sprouts in a given field of view vary in their stage of migration, it wouldn't make sense to calculate a frequency of this

detachment due to this time dependency. We have therefore removed the term “often” from our original sentence.

We did, however, further analyze how the abandoned WT ECs behaved after detachment of the leading mutant EC. We have now added this quantification in Extended Data Fig. 7 (also shown below). We found that from the 26 identified cases of mutant EC detachment in mosaic sprouts, stalk WT ECs retracted or arrested migration in 20 of the cases. Most importantly, to then show that the WT ECs were brought forward due to cell-cell forces, we then used our novel extension of 3D TFM to confirm pulling forces at the interface in Fig. 3h.

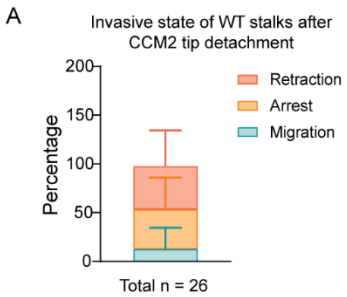

Extended Data Fig. 7: Retracting frequency of WT ECs. Quantification of the percent categorical distribution of the invasive state of WT EC stalks after detachment of a leading CCM2 tip EC in CCM2 mutant mosaics. The total number of mosaic sprouts identified with detaching tips are 26. The number of cases showing retraction are 10, arrest in migration are 10, and continued migration are 6. (From timelapse imaging videos taken from 3 independent trials with 3 FOVs/trial).

The adapted text and the reference to this new figure is as follows in Lines 233 to 236:

> *“When observing invasion dynamics, we noted that hyper-migratory siCCM2 tip cells detached and invaded farther away from a WT stalk leaving it behind (Fig. 2c, 3g, Supplementary Video 3). Interestingly, the WT stalk seemed to either retract (Fig. 3g, white arrow) or decelerate migration (Fig. 3g, yellow arrow) after detachment of the siCCM2 tip cell (Extended Data Fig. 7).”*

9. In Discussion, consider exploring the possibility that CCM2-silenced cells exhibit increased adhesion, causing surrounding cells to adhere and move with them. This alternative hypothesis could provide a different perspective on the observed behaviors.

We have made an adaptation to the discussion to include this concept as follows in Lines 332 to 343:

> *“Our findings demonstrate that the aggravation of force exertion on the ECM by CCM2 mutants can be felt by follower wild type ECs. While it is plausible that there is always force transmission between tip and stalk cells to sustain collective migration during physiological sprouting, the substantial increase in cell-ECM forces due to CCM2 mutants suggest that any force transmission between a mutant leader and a follower would likely be amplified, given also the force equilibrium boundary conditions. Unfortunately, quantifying and comparing this phenomenon in our model was impossible because wild type ECs rarely formed mosaic sprouts with control ECs, and they never occupied stalk positions behind them. This even suggested a complete lack of physical intercellular communication between populations in CT mosaics. Importantly, the proposed mechanism of hypercontractile mutants pulling forward passive*

wild type ECs was also associated with the reinforcement of the actin cytoskeleton and β1 focal adhesions in follower WT ECs. While it is also possible that cell-cell adhesions between CCM2 mutants and WT ECs are strengthened to promote this force transmission, the weakening of cell-cell junctions previously observed in CCM1/2-silenced EC 2D monolayers contradicts this idea [45]. However, the junctional adhesion strength has not yet been explored between mutant and non-mutant ECs."

10. In Discussion, it would be beneficial to critically evaluate whether the observed phenomena should be characterized as mechanical signals or simply as a result of physical forces. This distinction is important for accurately interpreting the study's findings.

We assume the reviewer is referring to the word mechanical signaling in Line 368 which is indeed ambiguous. We have now rewritten the sentence as follows:

"*How cell-cell forces are then transmitted to the nucleus to activate a reprogramming remains to be explored*."

In addition, we have adapted the discussion to clarify this as it pertains to our findings in Lines 344 to 350 as follows:

"*We speculate that a mechanical continuum is established between the cytoskeletal machinery of the mutants and wild-type ECs, although the underlying mechanisms remain to be addressed. It is conceivable that localized high forces at mosaic cell-cell junctions induce a force-dependent global activation of signaling resulting in increased active β1 integrins and actin assembly in WT ECs. This is similar to the reinforcement of β1 integrin-dependent adhesive structures observed in response to PECAM mechanical activation involving PI3K and Rho signaling pathways[50]. Besides enabling focal adhesions and invasion, CCM2 mutants also initiate a transcriptomic reprogramming of wild type ECs into a stalk-like identity, characterized by the downregulation of tip cell markers and the upregulation of matrix deposition genes.*"

BIBLIOGRAPHY

1. Pagenstecher, A., Stahl, S., Sure, U. & Felbor, U. A two-hit mechanism causes cerebral cavernous malformations: complete inactivation of CCM1, CCM2 or CCM3 in affected endothelial cells. *Hum Mol Genet* **18**, 911–918 (2009).

2. Snellings, D. A. *et al.* Cerebral Cavernous Malformation: From Mechanism to Therapy. *Circ Res* **129**, 195–215 (2021).

3. Malinverno, M. *et al.* Endothelial cell clonal expansion in the development of cerebral cavernous malformations. *Nat Commun* **10**, 2761 (2019).

4. Gault, J. *et al.* Cerebral Cavernous Malformations: Somatic Mutations in Vascular Endothelial Cells. *Neurosurgery* **65**, 138 (2009).

5. Gault, J., Shenkar, R., Recksiek, P. & Awad, I. A. Biallelic Somatic and Germ Line CCM1 Truncating Mutations in a Cerebral Cavernous Malformation Lesion. *Stroke* **36**, 872–874 (2005).

6. Akers, A. L., Johnson, E., Steinberg, G. K., Zabramski, J. M. & Marchuk, D. A. Biallelic somatic and germline mutations in cerebral cavernous malformations (CCMs): evidence for a two-hit mechanism of CCM pathogenesis. *Hum Mol Genet* **18**, 919–930 (2009).

7. Vannier, D. R. *et al.* CCM2-deficient endothelial cells undergo a ROCK-dependent reprogramming into senescence-associated secretory phenotype. *Angiogenesis* **24**, 843–860 (2021).

8. De Smet, F., Segura, I., De Bock, K., Hohensinner, P. J. & Carmeliet, P. Mechanisms of Vessel Branching. *Arterioscler Thromb Vasc Biol* **29**, 639–649 (2009).

9. Fischer, R. S., Lam, P. Y., Huttenlocher, A. & Waterman, C. M. Filopodia and focal adhesions: An integrated system driving branching morphogenesis in neuronal pathfinding and angiogenesis. *Dev Biol* **451**, 86–95 (2019).

10. Barrasa-Fano, J. *et al.* TFMLAB: A MATLAB toolbox for 4D traction force microscopy. *SoftwareX* **15**, 100723 (2021).

11. Sanz-Herrera, J. A., Barrasa-Fano, J., Cóndor, M. & Van Oosterwyck, H. Inverse method based on 3D nonlinear physically constrained minimisation in the framework of traction force microscopy. *Soft Matter* **17**, 10210–10222 (2021).

12. Barrasa-Fano, J. *et al.* Advanced in silico validation framework for three-dimensional traction force microscopy and application to an in vitro model of sprouting angiogenesis. *Acta Biomater* **126**, 326–338 (2021).

13. Maruthamuthu, V., Sabass, B., Schwarz, U. S. & Gardel, M. L. Cell-ECM traction force modulates endogenous tension at cell-cell contacts. *Proc Natl Acad Sci U S A* **108**, 4708–4713 (2011).

14. Steinwachs, J. *et al.* Three-dimensional force microscopy of cells in biopolymer networks. *Nat Methods* **13**, 171–176 (2016).

15. Plotnikov, S. V., Sabass, B., Schwarz, U. S. & Waterman, C. M. High-Resolution Traction Force Microscopy. *Methods Cell Biol* **123**, 367 (2014).

16. Butler, J. P., Toli-Nørrelykke, I. M., Fabry, B. & Fredberg, J. J. Traction fields, moments, and strain energy that cells exert on their surroundings. *Am J Physiol Cell Physiol* **282**, (2002).

17. Newell-Litwa, K. A. *et al.* ROCK1 and 2 differentially regulate actomyosin organization to drive cell and synaptic polarity. *Journal of Cell Biology* **210**, 225–242 (2015).

18. Shirley, M. D. *et al.* Sturge–Weber Syndrome and Port-Wine Stains Caused by Somatic Mutation in GNAQ . *New England Journal of Medicine* **368**, 1971–1979 (2013).

19. Hammill, A. M. & Boscolo, E. Capillary malformations. *J Clin Invest* **134**, (2024).

20. Mäkinen, T., Boon, L. M., Vikkula, M. & Alitalo, K. Lymphatic Malformations: Genetics, Mechanisms and Therapeutic Strategies. *Circ Res* **129**, 136–154 (2021).

21. Kobialka, P. *et al.* The onset of PI3K-related vascular malformations occurs during angiogenesis and is prevented by the AKT inhibitor miransertib. *EMBO Mol Med* **14**, (2022).

22. Choi, E. J. *et al.* Enhanced Responses to Angiogenic Cues Underlie the Pathogenesis of Hereditary Hemorrhagic Telangiectasia 2. *PLoS One* **8**, e63138 (2013).

23. Snellings, D. A. *et al.* Somatic Mutations in Vascular Malformations of Hereditary Hemorrhagic Telangiectasia Result in Bi-allelic Loss of ENG or ACVRL1. *Am J Hum Genet* **105**, 894 (2019).

24. Detter, M. R. *et al.* Novel Murine Models of Cerebral Cavernous Malformations. *Angiogenesis* **23**, 651–666 (2020).

25. Rath, M., Pagenstecher, A., Hoischen, A. & Felbor, U. Postzygotic mosaicism in cerebral cavernous malformation. *J Med Genet* **57**, 212–216 (2020).

26. Luks, V. L. *et al.* Lymphatic and Other Vascular Malformative/Overgrowth Disorders Are Caused by Somatic Mutations in PIK3CA. *J Pediatr* **166**, 1048-1054.e5 (2015).

27. Detter, M. R., Snellings, D. A. & Marchuk, D. A. Cerebral cavernous malformations develop through clonal expansion of mutant endothelial cells. *Circ Res* **123**, 1143–1151 (2018).

28. Zhao, Q. *et al.* Single-cell transcriptome analyses reveal endothelial cell heterogeneity in tumors and changes following antiangiogenic treatment. *Cancer Res* **78**, 2370–2382 (2018).

29. Rosano, S. *et al.* A regulatory microRNA network controls endothelial cell phenotypic switch during sprouting angiogenesis. *Elife* **9**, (2020).

30. Vaeyens, M. M. *et al.* Matrix deformations around angiogenic sprouts correlate to sprout dynamics and suggest pulling activity. *Angiogenesis* **23**, 315–324 (2020).

31. Thomsen, M. S., Routhe, L. J. & Moos, T. The vascular basement membrane in the healthy and pathological brain. *Journal of Cerebral Blood Flow & Metabolism* **37**, 3300 (2017).

32. Ludwig, B. S., Kessler, H., Kossatz, S. & Reuning, U. RGD-Binding Integrins Revisited: How Recently Discovered Functions and Novel Synthetic Ligands (Re-)Shape an Ever-Evolving Field. *Cancers 2021, Vol. 13, Page 1711* **13**, 1711 (2021).

33. Pedchenko, V., Zent, R. & Hudson, B. G. αvβ3 and αvβ5 Integrins Bind Both the Proximal RGD Site and Non-RGD Motifs within Noncollagenous (NC1) Domain of the α3 Chain of Type IV Collagen: IMPLICATION FOR THE MECHANISM OF ENDOTHELIAL CELL ADHESION *. *Journal of Biological Chemistry* **279**, 2772–2780 (2004).

34. Renz, M. *et al.* Regulation of β1 Integrin-Klf2-Mediated Angiogenesis by CCM Proteins. *Dev Cell* **32**, 181–190 (2015).

35. Faurobert, E. *et al.* CCM1-ICAP-1 complex controls ??1 integrin-dependent endothelial contractility and fibronectin remodeling. *Journal of Cell Biology* **202**, 545–561 (2013).

36. Hong, C. C. *et al.* Cerebral cavernous malformations are driven by ADAMTS5 proteolysis of versican. *J Exp Med* **217**, (2020).

37. Patterson, J. & Hubbell, J. A. Enhanced proteolytic degradation of molecularly engineered PEG hydrogels in response to MMP-1 and MMP-2. *Biomaterials* **31**, 7836–7845 (2010).

38. Jauhiainen, S. *et al.* Proteomics on human cerebral cavernous malformations reveals novel biomarkers in neurovascular dysfunction for the disease pathology. (2024) doi:10.1016/j.bbadis.2024.167139.

39. Fujimura, M., Watanabe, M., Shimizu, H. & Tominaga, T. Expression of matrix metalloproteinases (MMPs) and tissue inhibitor of metalloproteinase (TIMP) in cerebral cavernous malformations: Immunohistochemical analysis of MMP-2, -9 and TIMP-2. *Acta Neurochir (Wien)* **149**, 179–183 (2007).

40. Kraning-Rush, C. M., Carey, S. P., Lampi, M. C. & Reinhart-King, C. A. Microfabricated collagen tracks facilitate single cell metastatic invasion in 3D. *Integr Biol (Camb)* **5**, 606 (2013).

41. Bordeleau, F. *et al.* Matrix stiffening promotes a tumor vasculature phenotype. *Proc Natl Acad Sci U S A* **114**, 492–497 (2017).

42. Raeber, G. P., Lutolf, M. P. & Hubbell, J. A. Molecularly Engineered PEG Hydrogels: A Novel Model System for Proteolytically Mediated Cell Migration. *Biophys J* **89**, 1374–1388 (2005).

43. Adrian, E. *et al.* Complexation of cxcl12, fgf-2 and vegf with heparin modulates the protein release from alginate microbeads. *Int J Mol Sci* **22**, 11666 (2021).

44. Julian, L. & Olson, M. F. Rho-associated coiled-coil containing kinases (ROCK). *Small GTPases* **5**, e29846 (2014).

45. Lisowska, J. *et al.* The CCM1-CCM2 complex controls complementary functions of ROCK1 and ROCK2 that are required for endothelial integrity. *J Cell Sci* **131**, jcs.216093 (2018).

46. Ayata, C. *et al.* Role of Rho-Associated Kinase in the Pathophysiology of Cerebral Cavernous Malformations. *Neurol Genet* (2024) doi:10.1212/NXG.0000000000200121.

47. Wang, Y. & McNiven, M. A. Invasive matrix degradation at focal adhesions occurs via protease recruitment by a FAK-p130Cas complex. *J Cell Biol* **196**, 375–385 (2012).

48. Niland, S., Riscanevo, A. X. & Eble, J. A. Matrix Metalloproteinases Shape the Tumor Microenvironment in Cancer Progression. *International Journal of Molecular Sciences 2022, Vol. 23, Page 146* **23**, 146 (2021).

49. Van Hinsbergh, V. W. M. & Koolwijk, P. Endothelial sprouting and angiogenesis: matrix metalloproteinases in the lead. *Cardiovasc Res* **78**, 203–212 (2008).

50. Collins, C. *et al.* Localized Tensional Forces on PECAM-1 Elicit a Global Mechanotransduction Response via the Integrin-RhoA Pathway. *Current Biology* **22**, 2087–2094 (2012).

REVIEWERS' COMMENTS

Reviewer #1 (Remarks to the Author):

The authors have responded very thoroughly and thoughtfully to all of my comments. They have then incorporated new data and new text to clarify the issues that I brought up. I am pleased with the final results and believe this to be a very strong and interesting paper.

Reviewer #2 (Remarks to the Author):

Overview:

I reviewed the revised manuscript titled "Force-mediated recruitment and reprogramming of healthy endothelial cells drive vascular lesion growth" by Shapeti et al. and would like to thank the authors for their diligent efforts to address the concerns and suggestions outlined in my initial review. Below, I detail my assessment of the revisions and my recommendation for the manuscript's publication.

General Assessment:
The authors have comprehensively addressed most of the issues that were raised in my initial review. The revisions made to the manuscript have significantly improved the clarity, accuracy, and overall quality of the work. Specifically, I appreciate the efforts made to clarify the methodology section and expand on the introduction and discussion to make it clearer. However, I still hold a concern about their sample sizes, raised in my initial Major Concern 5. Two independent experiments are not a commonly-accepted experimental design in the field. Minor suggestion: Please add the scale bar for Figure 1.

Conclusion:
In light of the revisions made and the authors' responsiveness to feedback, I believe that the manuscript has been improved substantially. The work represents a valuable contribution to the field. However, given the concerns about sample size, I still have reservations in that regard. In balance, I am willing to recommend the paper be accepted in its present form.

Reviewer #3 (Remarks to the Author):

I co-reviewed this manuscript with one of the reviewers who provided the listed reports. This is part of the Nature Communications initiative to facilitate training in peer review and to provide appropriate recognition for Early Career Researchers who co-review manuscripts.